天主教輔仁大學物理學系碩士論文

指導教授 ： 張敏娟 教授

在 Belle II 實驗中尋找 B^0 介子衰變至 $J/\psi\eta$ 之分析

The study of B^0 to $J/\psi\eta$ in Belle II Experiment at KEK

研究生 ： 許員豪 撰

中華民國 一百一十年一月

The study of B^0 to $J/\psi\eta$ in Belle II Experiment at KEK

M.C. Chang, Y.H. Hsu

Fu-Jen Catholic University

January 20, 2021

摘要

在本論文中，我們在 Belle II 實驗的環境，利用蒙地卡羅方法，產生我們預期的稀有衰變$B^0 \to J/\psi\eta$來做物理事件模擬，並藉由 Belle II 的軟體分析模組 (basf2)，我們對模擬的物理事件進行篩選，再利用日本高能加速器研究機構(KEK)裡的正負電子對撞機(KEKB)所產生的 B 介子，進行物理事件的分析。在 KEKB 中所產生的 B 介子是利用 Belle 偵測器所蒐集的，其所蒐集的 B 介子總事件數為七億七千一百萬個(771M)。我們利用 Belle 實驗所產生的物理事件透過 B2BII 模組轉換資料格式進行分析，得到$B^0 \to J/\psi\eta$的衰變率為$(10.9 \pm 1.6 \pm 1.2)\times 10^{-6}$，顯著度為 8.7σ。其中，衰變率中的 1.6 為統計誤差，1.2 為系統誤差。此研究的衰變率結果，與 Belle 之前發表的兩篇論文一致。本分析方法與之前不同的地方在於，本研究使用的是 Belle II 的偵測器模擬，而非 Belle 的。變數最佳化的選擇也是根據 Belle II 偵測器的環境，衰變率顯著度稍微提升，但誤差也提升了。

關鍵詞：日本高能加速器研究機構，Belle 實驗，Belle II 實驗，B 介子稀有衰變

Abstract

We study the decay of $B^0 \to J/\psi\eta$ based on the Belle data samples at the $\Upsilon(4S)$ resonance and compare to the results in PRL 2007 "Observation of the Decay $B^0 \to J/\psi\eta$ " [1] and PRD 2012 "Measurement of $B^0 \to J/\psi\eta^{(\prime)}$ and constraint on the $\eta - \eta'$ mixing angle" [2]. The branching fraction is $(9.5 \pm 1.7 \pm 0.8) \times 10^{-6}$ and the significance 8.1σ in PRL 2007. The branching fraction is $\left(12.3 \pm {}^{1.8}_{1.7} \pm 0.7\right) \times 10^{-6}$ and the significance is 6.3σ in PRD 2012.

In this study, we use the Monte Carlo method to generate the expected rare decay $B^0 \to J/\psi\eta$ in the environment of the Belle II experiment for physical event simulation and use the Belle II software analysis module (basf2). The B mesons are generated by the electron-position collider (KEKB) in the High Energy Accelerator Research Organization (KEK) and collected by Belle Detector. The total number of $B\bar{B}$ events are 771 million. We convert the Belle mdst to Belle II mdst by the module B2BII. The branching fraction of $B^0 \to J/\psi\eta$ in our study is $(10.9 \pm 1.6 \pm 1.2) \times 10^{-6}$. The significance is 8.7σ. The difference between this analysis method and the previous two published results is that this study uses the Belle II detector simulation instead of Belle's. The optimize selections of variables are also based on the environment of the Belle II detector. The significance of the branching fraction in this study is increased a bit, but the errors are also increased a bit.

Keyword: KEK, Belle Experiment, Belle II Experiment, B decay

致謝

時光飛逝，兩年多的碩士研究生涯也接近尾聲，首先我要先感謝我的指導教授張敏娟老師，在張敏娟老師的耐心指導下，才得以順利的完成此研究，在研究的過程中遇到困難時，張敏娟老師總是能提供給我不同的思考切入點，讓我試著協助從不同面向來解決困難。除此之外，也感謝我的口試委員—張寶棣老師以及王名儒老師，在口試的過程中，提點出我在研究過程中的盲點。另外我也要感謝在台灣大學的黃坤賢學長，在剛踏入高能研究的領域的我，仍耐心的教導我們如何在 Belle II 環境做研究，以及冠宇學弟的協助。也感謝家庭、朋友的幫忙、支持與鼓勵，讓我得以專心地完成研究。

Context

CHAPTER 1 INTRODUCTION 1

1.1 MOTIVATION 1

1.2 FEYNMAN DIAGRAM 2

CHAPTER 2 EVENT GENERATION, SIMULATION AND SELECTION 3

2.1 ANALYSIS TOOLS 3

2.1.1 Belle II Analysis Software Framework 3

2.1.2 EvtGen 4

2.1.3 ROOT 5

2.1.4 B2BII 6

2.2 EVENT GENERATION 8

2.2.1 Decay Table 8

2.2.2 Event Generation 11

2.3 B MESON RECONSTRUCTION 12

2.3.1 Tracking 12

2.3.2 Particle Identification 13

2.3.3 Requirements for reconstructed J/ψ 14

2.3.4 Requirements for the reconstructed η 19

2.3.5 Requirements for reconstructed B^0 25

2.3.6 Signal PDF 28

CHAPTER 3 BACKGROUND 30

3.1 BACKGROUND SURVEY 30

3.1.1 Background Monte Carlo Event Type 30

3.1.2 $\boldsymbol{R_2}$ Definition 31

3.1.3 Backgrounds 32

3.2 BACKGROUND PDF 34

3.3 CONTROL SAMPLE 36

3.4 TOY MC & PULL TEST 40

CHAPTER 4 SYSTEMATIC ERRORS 47

4.1 OFFICIAL SYSTEMATIC ERRORS 47

4.1.1 Tracking 47

4.1.2 Number of $\boldsymbol{B\bar{B}}$ events 47

4.1.3 KID selection 47

4.1.4 Lepton selection 49

4.2 $\boldsymbol{J/\psi}$ SELECTION 54

4.3 $\boldsymbol{\eta}$ SELECTION 56

4.4 FITTING 57

4.5 SUMMARY OF THE SYSTEMATIC ERRORS 60

CHAPTER 5 OPEN DATA BOX 61

5.1 BELLE DATA 61

5.2 BELLE II DATA 63

CHAPTER 6 SUMMARY 64

6.1 THE BRANCHING FRACTION OF $B^0 \to J/\psi\eta$ 64

6.2 RESULT COMPARISON 65

APPENDIX A. BELLE DATA 66

APPENDIX B. BELLE II DATA 68

APPENDIX C. BELLE II ANALYSIS SOFTWARE FRAMEWORK 69

RELEASE-04-02-04 69

LIGHT-2002-JANUS 69

1. BremsFinder 69

參照 70

List of Figures

Fig 2.1 Modules and paths of the Belle II Analysis Software Framework. [3] 3
Fig 2.2 Example of a basf2 steering file 4
Fig 2.3 Design philosophy of RooFit related to the mathematical concept. 5
Fig 2.4 Schematic view of the conversion process of Belle (light blue) to Belle II (blue) mDST files using the BASF2 modules (gray) provided by the b2bii package and the original Belle software provided by the belle_legacy library (gray). 6
Fig 2.5 Matching of the Belle PANTHER Tables (light blue) to the Belle II ROOT objects (blue) and relations (orange). 7
Fig 2.6 Decay table of $B^0 \to J/\psi\eta(J/\psi \to e^+e^-\ (\gamma),\ \eta \to \gamma\gamma)$ mode 8
Fig 2.7 Decay table of $B^0 \to J/\psi\eta(J/\psi \to e^+e^-(\gamma),\ \eta \to \pi^+\pi^-\pi^0)$mode. 9
Fig 2.8 Decay table of $B^0 \to J/\psi\eta(J/\psi \to \mu^+\mu^-,\ \eta \to \gamma\gamma)$mode 10
Fig 2.9 Decay table of $B^0 \to J/\psi\eta(J/\psi \to \mu^+\mu^-,\ \eta \to \pi^+\pi^-\pi^0)$mode . 11
Fig 2.10 Belle II Top View 13
Fig 2.11 The $M_{J/\psi}$ of the decay channel $J/\psi \to\ e^+e^-(\gamma), \eta \to \gamma\gamma$ 16
Fig 2.12 The $M_{J/\psi}$ of the decay channel $J/\psi \to e^+e^-(\gamma),\ \eta \to \pi^+\pi^-\pi^0$ 16
Fig 2.13 The $M_{J/\psi}$ of the decay channel $J/\psi \to \mu^+\mu^-, \eta \to \gamma\gamma$ 18
Fig 2.14 The $M_{J/\psi}$ of the decay channel $J/\psi \to \mu^+\mu^-, \eta \to \pi^+\pi^-\pi^0$ 18
Fig 2.16 The M_η of the decay channel $J/\psi \to e^+e^-(\gamma), \eta \to \gamma\gamma$ 20
Fig 2.17 The M_η of the decay channel $J/\psi \to \mu^+\mu^-, \eta \to \gamma\gamma$ 20
Fig 2.18 The M_η of the decay channel $J/\psi \to e^+e^-(\gamma), \eta \to \pi^+\pi^-\pi^0$ 22
Fig 2.19 The M_η of the decay channel $J/\psi \to \mu^+\mu^-, \eta \to \pi^+\pi^-\pi^0$ 23
Fig 2.20 The M_{π^0} of the decay channel $J/\psi \to e + e - \gamma, \eta \to \pi^+\pi^-\pi^0$. 23
Fig 2.21 The M_{π^0} of the decay channel $J/\psi \to \mu^+\mu^-, \eta \to \pi^+\pi^-\pi^0$ 24
Fig 2.22 ΔE and M_{bc} distributions of decay mode $J/\psi \to e^+e^-(\gamma), \eta\ \to \gamma\gamma$ 26
Fig 2.23 ΔE and M_{bc} distributions of decay mode $J/\psi \to e^+e^-(\gamma), \eta\ \to \pi^+\pi^-\pi^0$ 26

Fig 2.24 ΔE and M_{bc} distributions of decay mode $J/\psi \to \mu^+\mu^-, \eta \to \gamma\gamma$ 27
Fig 2.25 ΔE and M_{bc} distributions of decay mode $J/\psi \to \mu^+\mu^-, \eta \to \pi^+\pi^-\pi^0$ 27
Fig 2.26 The signal PDF of ΔE distribution in the decay mode $J/\psi \to l^+l^-, \eta \to \gamma\gamma$ 28
Fig 2.27 The signal PDF of ΔE distribution in the decay mode $J/\psi \to l^+l^-, \eta \to \pi^+\pi^-\pi^0$ 29
Fig 3.1 The background PDFs of ΔE distribution in decay channel $J/\psi \to l^+l^-, \eta \to \gamma\gamma$ 34
Fig 3.2 The background PDF of ΔE distribution combined qq and bb for decay channel $J/\psi \to l^+l^-, \eta \to \gamma\gamma$ 34
Fig 3.3 The background PDFs of ΔE distribution in decay channel $J/\psi \to l^+l^-, \eta \to \pi^+\pi^-\pi^0$ 35
Fig 3.4 The background PDF of ΔE combined qq and bb for decay channel $J/\psi \to l^+l^-, \eta \to \pi^+\pi^-\pi^0$ 35
Fig 3.5 The signal PDF of ΔE distribution in control sample $B^\pm \to J/\psi K^{*+}(892), (J/\psi \to l^+l^-)(K^{*+} \to K^\pm\pi^0)$ 37
Fig 3.6 ΔE distribution of control sample $B^\pm \to J/\psi K^{*+}(892), (J/\psi \to l^+l^-)(K^{*+} \to K^\pm\pi^0)$ use Belle II Data..... 38
Fig 3.7 ΔE distribution of control sample $B^\pm \to J/\psi K^{*+}(892), (J/\psi \to l^+l^-)(K^{*+} \to K^\pm\pi^0)$use Belle Data..... 38
Fig 3.8 The concept of calculating the number of backgrounds event in the signal yield region. 42
Fig 3.9 The toy test fitting plot of the $\eta \to \gamma\gamma$ decay mode..... 44
Fig 3.10 The PULL Test of the $\eta \to \gamma\gamma$ decay mode..... 45
Fig 3.11 The toy test fitting plot of the $\eta \to \pi^+\pi^-\pi^0$ decay mode..... 45
Fig 3.12 The PULL Test of the $\eta \to \pi^+\pi^-\pi^0$ decay mode..... 46
Fig 4.1 The ΔE distribution due to J/ψ decay angle selection on the control sample of $J/\psi\ K^{*+}$ in Monte Carlo..... 54
Fig 4.2 The ΔE distribution due to J/ψ decay angle selection on the control sample of $J/\psi\ K^{*+}$ in the Belle Data 55

Fig 4.3 The ΔE distribution fitting result of the control sample when the mean value adds 1σ. 57
Fig 4.4 The ΔE distribution fitting result of the control sample when the mean value subtracts 1σ..... 58
Fig 4.5 The ΔE distribution fitting result of the control sample with the widen width of 1.5σ. 58
Fig 4.6 The ΔE distribution fitting result of the control sample with the narrowed width of 0.5σ..... 59
Fig 5.1 The ΔE distribution fitting result of data in the $\eta \to \gamma\gamma$ decay. 63
Fig 5.2 The ΔE distribution fitting result of data in the $\eta \to \pi^+\pi^-\pi^0$ decay..... 63
Fig 6.1 The ΔE distribution result of the simultaneous fit in the $B^0 \to J/\psi\eta$ decay..... 65

List of Tables

Table 3.1 The number of generated events in the thirteenth official background Monte Carlo campaign (MC13) 30
Table 3.2 The main components of backgrounds in $B^0 \to J/\psi(e^+e^-(\gamma))\eta(\gamma\gamma)$ mode 32
Table 3.3 The main components of backgrounds in $B^0 \to J/\psi(e^+e^-(\gamma))\eta(\pi^+\pi^-\pi^0)$ mode. 32
Table 3.4 The main components of backgrounds in $B^0 \to J/\psi(\mu^+\mu^-)\eta(\gamma\gamma)$ mode. 33
Table 3.5 The main components of backgrounds in $B^0 \to J/\psi(\mu^+\mu^-)\eta(\pi^+\pi^-\pi^0)$ mode. 33
Table 3.6 The mean shift and the widen ratio of the signal PDF in control sample 39
Table 3.7 The number of signals in the signal yield region. 41
Table 3.8 The details of background number in the signal yield estimation for the decay $J/\psi \to e^+e^-(\gamma), \eta \to \gamma\gamma$ 43
Table 3.9 The details of background number in the signal yield estimation for the decay $J/\psi \to e^+e^-(\gamma), \eta \to \pi^+\pi^-\pi^0$ 43
Table 3.10 The details of background number in the signal yield estimation for the decay $J/\psi \to \mu^+\mu^-, \eta \to \gamma\gamma$ 43
Table 3.11 The details of background number in the signal yield estimation for the decay $J/\psi \to \mu^+\mu^-, \eta \to \pi^+\pi^-\pi^0$ 44
Table 3.12 The mean and sigma of PULL test. 46
Table 4.1 The Correction of the efficiency and the systematic error from KID 48
Table 4.2 The lepton ID for $e^{\pm}$ correction file related to the experiment number of Belle data. 49
Table 4.3 The lepton ID for $\mu^{\pm}$ correction file related to the experiment number of Belle data. 49
Table 4.4 The efficiency correction and the systematic error for e^+. 50
Table 4.5 The efficiency correction and the systematic error for e^-. 50
Table 4.6 The efficiency correction and the systematic error for μ^+. 51

Table 4.7 The efficiency correction and the systematic error for μ^-. 53
Table 4.8 The ratio of with and without decay angle selection and systematic error between Monte Carlo and Data for J/ψ selection.....55
Table 4.9 The event ratio between without E_γ selection and with $E_\gamma > 0.2\ GeV$ selection in Monte Carlo and Data for $\eta \to \gamma\gamma$ selection. 56
Table 4.10 The event ratio between without p_{π^0} selection and with $p_{\pi^0} > 0.2 GeV/c$ selection in Monte Carlo and Data for $\pi^0 \to \gamma\gamma$ selection.....56
Table 4.11 The systematic error tables for $J/\psi\eta$.....60
Table 5.1 The branching fraction listed for each meson which get from PDG Website.....61
Table 5.2 The signal efficiency for each decay channel.....62
Table 5.3 The signal yield, branching fraction and significance result for the $B^0 \to J/\psi\eta$ decay.....62
Table 6.1 The signal yield, branching fraction and the significance of $B^0 \to J/\psi\eta$ decay.....64
Table 6.2 The branching fraction comparison for PRL2007 PRD 2012 and this thesis.....65

Chapter 1 Introduction

1.1 Motivation

We are interested in the decay mode $B^0 \to J/\psi\,\eta$ which had been found in the Belle Experiment and the paper's titles are "Observation of the decay $B^0 \to J/\psi\,\eta$" and "Measurement of $B^0 \to J/\psi\,\eta^{(\prime)}$ and constraint on the $\eta - \eta'$ mixing angle".

In the former, the decay mode of $B^0 \to J/\psi\,\eta$ had been discovered based on the data sample with 449 million $B\bar{B}$ pairs accumulated at the $\Upsilon(4s)$ resonance with the Belle detector at the KEKB asymmetric energy e^+e^- collider. The signal is observed with a significance of 8.1σ and is obtained a branching fraction of $\left(9.5 \pm 1.7\ (stat) \pm 0.8(syst)\right) \times 10^{-6}$. [1]

In the later, the decay mode of $B^0 \to J/\psi\,\eta$ had been discovered based on the data sample with 771 million $B\bar{B}$ pairs accumulated at the $\Upsilon(4s)$ resonance with the Belle detector at the KEKB asymmetric energy e^+e^- collider. The signal is observed with a significance of 6.3σ and is obtained a branching fraction of $\left(12.3 \pm \frac{1.8}{1.7} \pm 0.7\right) \times 10^{-6}$. [2]

Result	Branching fraction	Significance	$N(B\bar{B})$
PRL 2007	$(9.5 \pm 1.7 \pm 0.8) \times 10^{-6}$	8.1σ	449M
RPD 2012	$\left(12.3 \pm \frac{1.8}{1.7} \pm 0.7\right) \times 10^{-6}$	6.3σ	771M

I study the decay mode $B^0 \to J/\psi\,\eta$ use the Belle Data and the Belle II Monte Carlo Simulation I want to know if I can observe the $B^0 \to J/\psi\,\eta$ using Belle II Data.

1.2 Feynman Diagram

Feynman diagram of B meson decay $B^0 \to J/\psi\eta$ is settled by the $\bar{b} \to \bar{c}c\bar{d}$ transition. This decay is a Cabibbo- and color-suppressed decay.

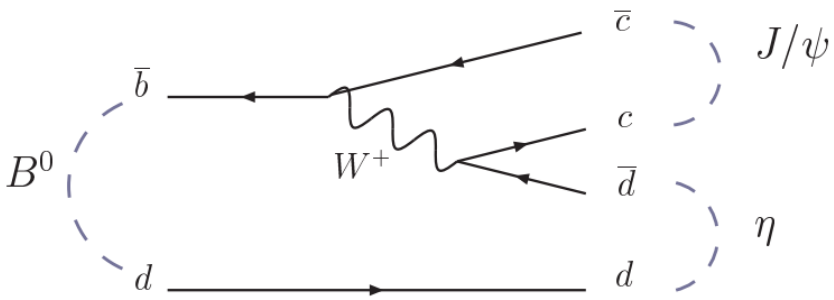

Fig 1.1 Feynman diagram for the leading contribution to the decay $B^0 \to J/\psi\eta$

Chapter 2 Event Generation, Simulation and Selection

2.1 Analysis Tools

2.1.1 Belle II Analysis Software Framework

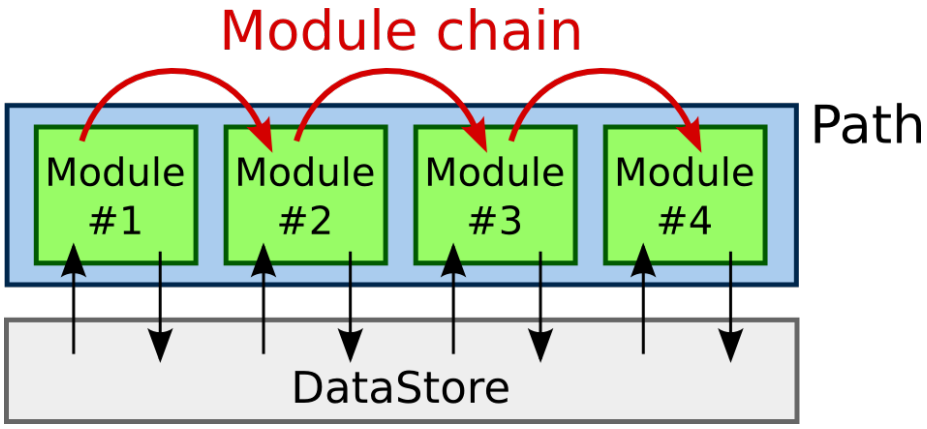

Fig 2.1 Modules and paths of the Belle II Analysis Software Framework. [3]

Belle II Analysis Software Framework (basf2) is the software framework to process the data from Belle II Experiment. The software is organized in the three parts: *basf2, externals,* and *tools*.

Basf2 is the Belle II-specific code which is partitioned into about 40 packages. The packages have modules, tools, dataobjects, script, data, etc. The base-level framework of basf2 is written in C++ and the scripts usually is written in Python. When we need to use the modules [3], we will load the library which is compiled by the tools and stored in the path "modules". The modules, their configuration, and their order of execution are defined via a Python Interface.[Fig 2.1][Fig 2.2] DataStore is the place where the module needs the data located at. The path is to arrange the module into the container as a series of the sequence for the modules executed.

Externals contains the third-party code for including the basic tools like GCC, Python3 to avoid requiring a system-wide installation and including the High Energy Physics specific software like ROOT, Geant4, and EvtGen. *Externals* provides the library and the environment for the needs of basf2.

Tools is a collection of shell and Python scripts for installing and setting up *basf2* and *externals*. Besides, *Tools* also provides the Belle II specific environment variables, defines functions for the setup, etc. The environment can be set up by sourcing *b2setup* to set up the specific software version for analyzing. [4]

```
#!/usr/bin/env python3
# -*- coding: utf-8 -*-

# Generate 100 events with event numbers 0 to 99↩
      that contain only the event meta data.

import basf2
main = basf2.create_path()
main.add_module('EventInfoSetter', evtNumList↩
    =[100])
basf2.process(main)
```

Fig 2.2 Example of a basf2 steering file

2.1.2 EvtGen

EvtGen is a physics Monte Carlo event generator designed for the simulation of the physics of B decays. EvtGen provides a framework to handle complex sequencial decays. It implements many decay models including semileptonic decays, hadronic decays, CP violating decays, angular distribution, and Dalitz decays. The EvtGen package provides a framework for implemention of physics processes relevant to decays of B mesons and other resonances. The individual physics processes are

implemented in modules that allow users to build complicated decays chains. [5] [6]

2.1.3 ROOT

ROOT is an object-oriented program originally developed by CERN designed for particle physics data analysis. The program and the library of ROOT is written in C++ but integrated with Python and R. ROOT provides the functionalities for dealing with big data processing, statistical analysis, visualization and storage. [7]

RooFit introduces a granular structure in its mapping of mathematical data models components to C++ objects: rather than aiming at a monolithic entity that describes a data model, each math symbol is presented by a separate object. A feature of this design philosophy is that all RooFit models always consist of multiple objects.. [8][Fig 2.3]

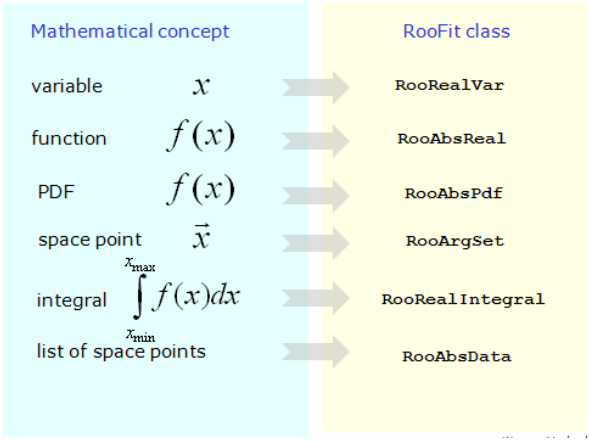

Fig 2.3 Design philosophy of RooFit related to the mathematical concept.

2.1.4 B2BII

The module “B2BII” provides the environment to analysis the belle data under the basf2 software.The Belle to Belle II dataset conversion converts the Belle mDST data, which contains mostly detector independent objects like tracks and calorimeter clusters, into the new mDST format used by BASF2. This enables the validation of the Belle II analysis software, and (re-)production of Belle measurements using the improved software. The conversion process is visualized in Fig 2.4.

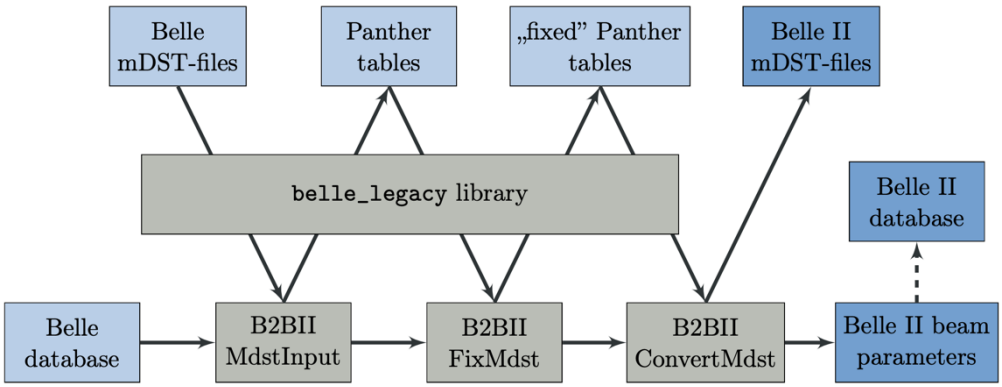

Fig 2.4 Schematic view of the conversion process of Belle (light blue) to Belle II (blue) mDST files using the BASF2 modules (gray) provided by the b2bii package and the original Belle software provided by the belle legacy library (gray).

The information defined between Belle and Belle II has some difference. The Fig 2.5shows the relation of variables between Belle and Belle II. [9]

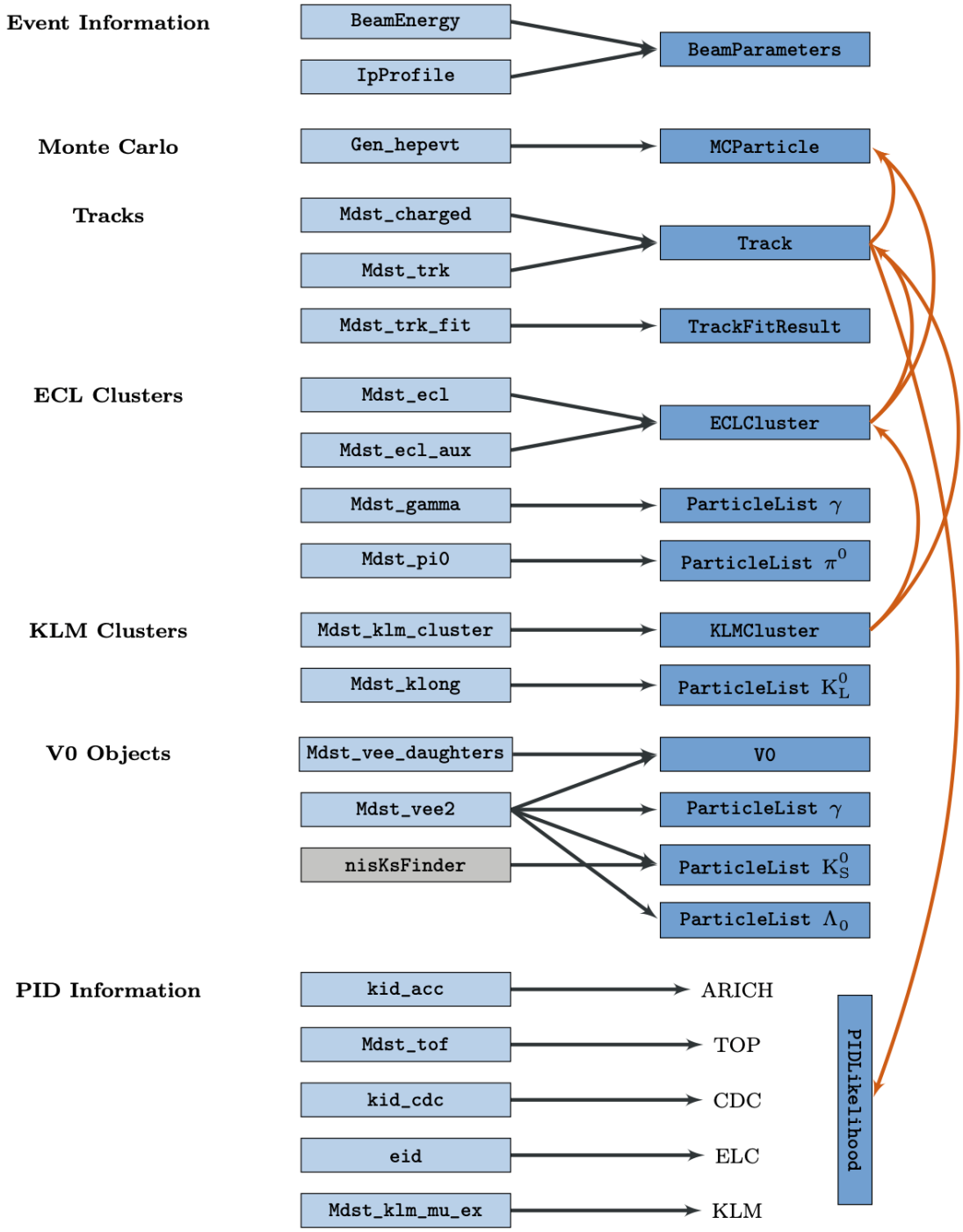

Fig 2.5 Matching of the Belle PANTHER Tables (light blue) to the Belle II ROOT objects (blue) and relations (orange).

2.2 Event Generation

2.2.1 Decay Table

The decay mode $B^0 \to J/\psi\eta$ has four different final states so we write four different decay tables. The J/ψ decays to e^+e^- and $\mu^+\mu^-$. The η decays to $\gamma\gamma$ and $\pi^+\pi^-\pi^0$. The decay tables are shown as [Fig 2.6][Fig 2.7][Fig 2.8][Fig 2.9]. In our signal Monte Carlo Simulation assumes 100% decay in each mode.

```
# EventType: 1111528000
# Descriptor: [B0 -> (J/psi(1S) -> e+ e-) (eta -> gamma gamma)]cc
# NickName: Bd_Jpsieta_ee_gg
# Documentation: CPV study, S=-sin(2 beta)=-0.691, A=0
# Tested: Yes
# Physics WG: TDCPV
# Responsible: Bilas Pal
# Email:  bilas.kanti.pal@desy.de
# Cuts: None
# Date: 20180326
#
#
Alias      etasig        eta
ChargeConj etasig        etasig
Define beta 0.3814
#
Decay Upsilon(4S)
1.0     B0sig anti-B0sig B0 anti-B0               VSS_BMIX dm;
Enddecay
#
Decay B0sig
1.000   J/psisig         etasig                       SVS_CP beta dm  1 1 0 1 0;
Enddecay
CDecay anti-B0sig
#
Decay etasig
1.000   gamma            gamma                        PHSP;
Enddecay
#
Decay J/psisig
1.000   e+               e-                           PHOTOS VLL;
Enddecay
#
End
```

Fig 2.6 Decay table of $B^0 \to J/\psi\eta(J/\psi \to e^+e^-(\gamma),\ \eta \to \gamma\gamma)$ mode

```
# EventType: 1111548000
# Descriptor: [B0 -> (J/psi(1S) -> e+ e-) (eta -> pi+ pi- pi0)]cc
# NickName: Bd_Jpsieta_ee_pipipi0
# Documentation: CPV study, S=-sin(2 beta)=-0.691, A=0
# Tested: Yes
# Physics WG: TDCPV
# Responsible: Bilas Pal
# Email:  bilas.kanti.pal@desy.de
# Cuts: None
# Date: 20180326
#
#
Alias      pi0sig        pi0
ChargeConj pi0sig        pi0sig
Alias      etasig        eta
ChargeConj etasig        etasig
Define beta 0.3814
#
Decay Upsilon(4S)
1.0     B0sig anti-B0sig B0 anti-B0               VSS_BMIX dm;
Enddecay
#
Decay B0sig
1.000   J/psisig         etasig                      SVS_CP beta dm  1 1 0 1 0;
Enddecay
CDecay anti-B0sig
#
Decay etasig
1.000   pi+    pi-       pi0sig                      PHSP;
Enddecay
#
Decay pi0sig
1.000   gamma            gamma                       PHSP;
Enddecay
#
Decay J/psisig
1.000   e+               e-                         PHOTOS VLL;
Enddecay
#
End
```

Fig 2.7 Decay table of $B^0 \to J/\psi\eta(J/\psi \to e^+e^-(\gamma),\ \eta \to \pi^+\pi^-\pi^0)$mode.

```
# EventType: 1111428000
# Descriptor: [B0 -> (J/psi(1S) -> mu+ mu-) (eta -> gamma gamma)]cc
# NickName: Bd_Jpsieta_mumu_gg
# Documentation: CPV study, S=-sin(2 beta)=-0.691, A=0
# Tested: Yes
# Physics WG: TDCPV
# Responsible: Bilas Pal
# Email:  bilas.kanti.pal@desy.de
# Cuts: None
# Date: 20180326
#
#
Alias      etasig        eta
ChargeConj etasig        etasig
Define beta 0.3814
#
Decay Upsilon(4S)
1.0     B0sig anti-B0sig B0 anti-B0               VSS_BMIX dm;
Enddecay
#
Decay B0sig
1.000   J/psisig         etasig                      SVS_CP beta dm  1 1 0 1 0;
Enddecay
CDecay anti-B0sig
#
Decay etasig
1.000   gamma            gamma                       PHSP;
Enddecay
#
Decay J/psisig
1.000   mu+              mu-                         PHOTOS VLL;
Enddecay
#
End
```

Fig 2.8 Decay table of $B^0 \to J/\psi\eta(J/\psi \to \mu^+\mu^-,\ \eta \to \gamma\gamma)$mode

```
# EventType: 1111448000
# Descriptor: [B0 -> (J/psi(1S) -> mu+ mu-) (eta -> pi+ pi- pi0)]cc
# NickName: Bd_Jpsieta_mumu_pipipi0
# Documentation: CPV study, S=-sin(2 beta)=-0.691, A=0
# Tested: Yes
# Physics WG: TDCPV
# Responsible: Bilas Pal
# Email:  bilas.kanti.pal@desy.de
# Cuts: None
# Date: 20180326
#
#
Alias      pi0sig        pi0
ChargeConj pi0sig        pi0sig
Alias      etasig        eta
ChargeConj etasig        etasig
Define beta 0.3814
#
Decay Upsilon(4S)
1.0     B0sig anti-B0sig B0 anti-B0               VSS_BMIX dm;
Enddecay
#
Decay B0sig
1.000   J/psisig         etasig                      SVS_CP beta dm  1 1 0 1 0;
Enddecay
CDecay anti-B0sig
#
Decay etasig
1.000   pi+    pi-       pi0sig                      PHSP;
Enddecay
#
Decay pi0sig
1.000   gamma             gamma                       PHSP;
Enddecay
#
Decay J/psisig
1.000   mu+               mu-                         PHOTOS VLL;
Enddecay
#
End
```

Fig 2.9 Decay table of $B^0 \to J/\psi\eta(J/\psi \to \mu^+\mu^-,\ \eta \to \pi^+\pi^-\pi^0)$mode

2.2.2 Event Generation

For each decay mode, we generate two million events for our Monte Carlo signal events. For running events, we separate them into 400 jobs. Each job generates five thousand events. The jobs are running at the KEKCC. The event generation is under the software version “release-04-02-04” of basf2.

2.3 B Meson Reconstruction

2.3.1 Tracking

The decay vertex of the B meson should be near the Interaction Point (IP). Therefore, we collect the information from pixelated silicon sensors (PXD), double-sided silicon strip sensors (SVD), and central drift chamber (CDC). Comparing to Belle Detector, the first two layers of PXD are closer to the interaction point, the radius of outermost layer VXD and the radius of CDC are both larger. PXD and SVD can measure the decay vertex position of B mesons and other particles. CDC measures the trajectories, momenta, and $\frac{dE}{dx}$ information of charged particles. The details of requirement are shown as below. [10] [11]

- The requirements for the charged particles of "good" tracking in basf2 are $|dr| < 0.5$ cm ,$|dz| <$ 2 cm, number of CDC hits associated to the track > 20 and the hits arewithin the acceptance angle of CDC. [12]

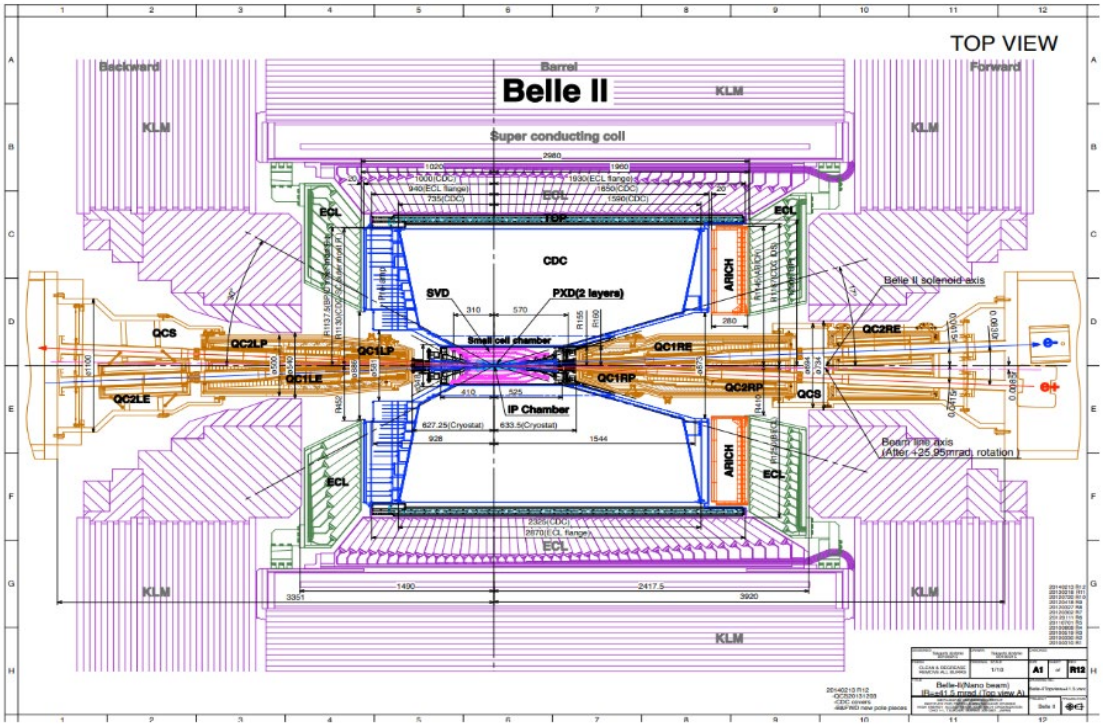

Fig 2.10 Belle II Top View

2.3.2 Particle Identification

For the particle identification, there are time-of-propagation counter (TOP) at the barrel region, ring-imaging Cherenkov Counters with aerogel (ARICH) at the forward end-cap region, electromagnetic calorimeter (ECL) and $K_L - Muon$ Detector (KLM). The ring-image of Cherenkov light cones emitted from charged particles passing through quartz radiator bars (TOP) and the aerogel radiator in the forward end-cap(ARICH).. ECL comprised of scintillator crystals, CsI(Tl), located inside a superconducting solenoid coil that provides 1.5T magnetic field. The ECL is used to detect gamma rays as well as to identify electrons, i.e. separate electrons from hadrons, in particular pions. [10] [11] [12]

- The requirements for the gammas of "loose" are $\theta_\gamma > 0.296706$, $\theta_\gamma < 2.61799$, $E > 50\ MeV$, and with the condition of $\frac{E_1}{E_9} > 0.4$ for ECL.

- The requirements for the gammas of "π^0" are $\theta_\gamma > 0.296706$, and $\theta_\gamma < 2.61799$.

- The particle identification probability of $e^\pm$ with"good" $\frac{\mathcal{L}_e}{(\mathcal{L}_e+\mathcal{L}_\mu+\mathcal{L}_\pi+\mathcal{L}_K+\mathcal{L}_p+\mathcal{L}_d)} > 0.5$

- The particle identification probability of $\mu^\pm$ with "good" $\frac{\mathcal{L}_\mu}{(\mathcal{L}_e+\mathcal{L}_\mu+\mathcal{L}_\pi+\mathcal{L}_K+\mathcal{L}_p+\mathcal{L}_d)} > 0.5$

- The particle identification probability of $\pi^\pm$ with "good" $\frac{\mathcal{L}_\pi}{(\mathcal{L}_e+\mathcal{L}_\mu+\mathcal{L}_\pi+\mathcal{L}_K+\mathcal{L}_p+\mathcal{L}_d)} > 0.5$

- For the particle in the Belle data selections, the PID of the particle $e^\pm$ is eIDBelle and the PID of the particle $\mu^\pm$ is muIDBelle.In my study, both of them should be larger than 0.4.

2.3.3 Requirements for reconstructed J/ψ

The J/ψ can be reconstructed by e^+e^- or $\mu^+\mu^-$. The "good" track is used to constrain the lepton e^+e^- and $\mu^+\mu^-$ from the standard particles library's "stdE" and "stdMu".

For the decay mode $J/\psi \rightarrow e^+e^-$, we set the constraint of reconstruction as following:

- Bremsstrahlung Photons : The photons which stay with 50 mrad of the e^+e^- track are counted. Besides, the energy of photons must be lower than 1.0 GeV

- Mass Window : $2.996\,\mathrm{GeV/c^2} < M_{e^+e^-(\gamma)} < 3.194\,\mathrm{GeV/c^2}$. We choose about 3σ width for the mass distribution. The PDG value of the mass J/ψ is $3.096916\ \mathrm{GeV/c^2}$ The mass distributions are shown in [Fig 2.11(b)] and [Fig 2.12(b)]. We choose the wider mass range of them.

- Fitting: Vertex Fit and Mass Fit.
  Vertex Fit: The leptons e^+e^- of J/ψcan be constrained with the charge tracks. The fitting technique is to obtain the vertices which is based on the least square method using the Lagrange multiplier method. [13]

  Mass Fit : The mass of J/ψin PDG value is $3.096916\ \mathrm{GeV/c^2}$. The Kfitter of Mass Fit is using invariant mass of J/ψ and the reoncstructed e^+e^- to do the fitting.
  We require the confidence level should be greater than 0 to reject the events which fail the fit of mass fit and vertex fit.
  After the fitting, the mass distribution of J/ψ are shown in [Fig 2.11(a)][Fig 2.12(a)].

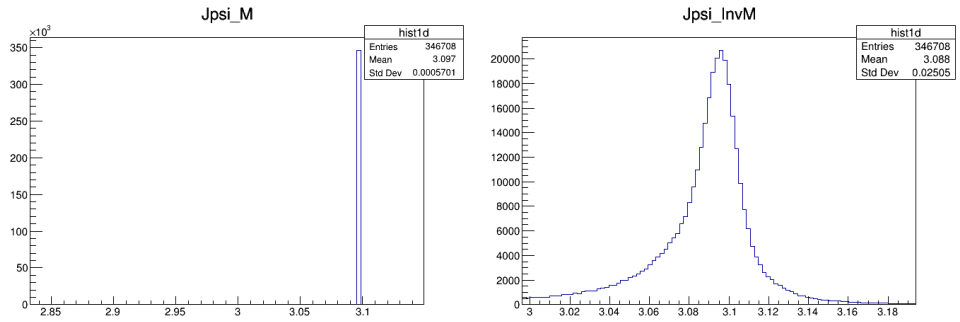

(a) Jpsi_M (left) : The $M_{J/\psi}$ distribution performed by vertex fitting.

(b) Jpsi_InvM (right) : The $M_{J/\psi}$ distribution determined by adding 4-momentum vectors of particle's daughter.

Fig 2.11 The $M_{J/\psi}$ of the decay channel $J/\psi \rightarrow e^+e^-(\gamma), \eta \rightarrow \gamma\gamma$

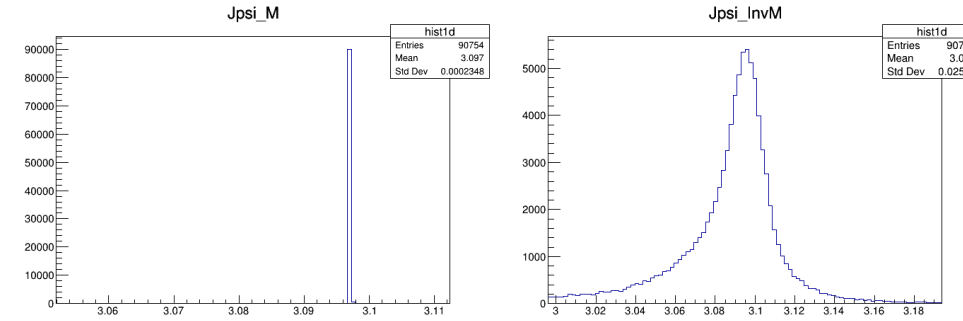

(a) Jpsi_M (left) : The $M_{J/\psi}$ distribution performed by vertex fitting.

(b) Jpsi_InvM (right) : The $M_{J/\psi}$ distribution determined by adding 4-momentum vectors of particle's daughter.

Fig 2.12 The $M_{J/\psi}$ of the decay channel $J/\psi \rightarrow e^+e^-(\gamma),\ \eta \rightarrow \pi^+\pi^-\pi^0$

For the decay mode $J/\psi \rightarrow \mu^+\mu^-$, we set the constraint of reconstruction as following.

- Mass Window: $3.029\ \mathrm{GeV/c^2} < M_{\mu^+\mu^-} < 3.165\ \mathrm{GeV/c^2}$ We choose about 3σ width for the mass distribution. The PDG value of the mass J/ψ is $3.096916\ \mathrm{GeV/c^2}$. The mass distributions are shown in [Fig 2.13 (b)] and [Fig 2.14 (b)]. We choose the wider mass range of them.

- Fitting: Vertex Fit and Mass Fit.
  Vertex Fit: The leptons $\mu^+\mu^-$ of J/ψcan be constrained with the charge tracks. The fitting technique is to obtain the vertices which is based on the least square method using the Lagrange multiplier method. [13]

  Mass Fit : The mass of J/ψin PDG value is $3.096916\ \mathrm{GeV/c^2}$. The Kfitter of Mass Fit is using invariant mass of J/ψ and the reoncstructed $\mu^+\mu^-$ to do the fitting.
  We require the confidence level should be greater than 0 to reject the events which fail the fit of mass fit and vertex fit.
  After the fitting, the mass distribution of J/ψ are shown in [Fig 2.13(a)][Fig 2.14 (a)].

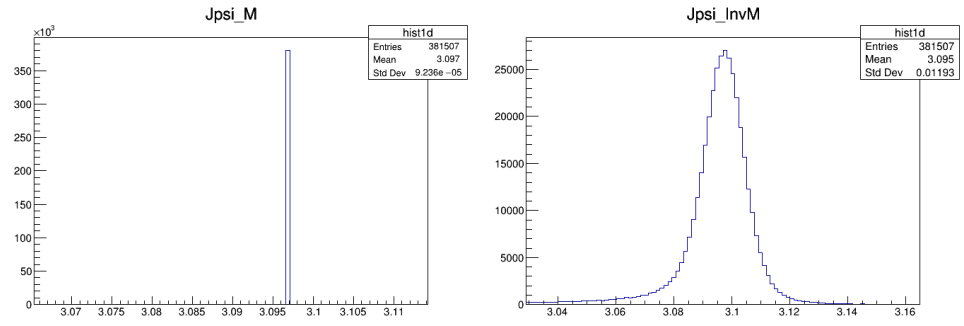

(a) Jpsi_M (left) : The $M_{J/\psi}$ distribution performed by vertex fitting.

(b) Jpsi_InvM (right) : The $M_{J/\psi}$ distribution determined by adding 4-momentum vectors of particle's daughter.

Fig 2.13 The $M_{J/\psi}$ of the decay channel $J/\psi \to \mu^+\mu^-, \eta \to \gamma\gamma$

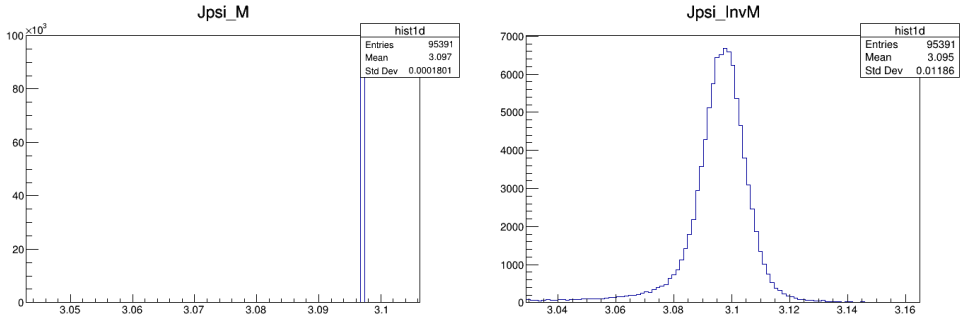

(a) Jpsi_M (left) : The $M_{J/\psi}$ distribution performed by vertex fitting.

(b) Jpsi_InvM (right) : The $M_{J/\psi}$ distribution determined by adding 4-momentum vectors of particle's daughter.

.

Fig 2.14 The $M_{J/\psi}$ of the decay channel $J/\psi \to \mu^+\mu^-, \eta \to \pi^+\pi^-\pi^0$

2.3.4 Requirements for the reconstructed η

There are two decay modes $\eta \to \gamma\gamma$ and $\eta \to \pi^+\pi^-\pi^0$ in our η reconstruction. Both of π^0 and η can decay to $\gamma\gamma$, therefore we need to require the mass and energy to identify them.

For the decay mode $\eta \to \gamma\gamma$, the selections are as follows.

- Energy of γ : $E_\gamma > 300MeV$

- Mass window of η: $495\ \mathrm{MeV/c^2} < M_\eta < 598\ \mathrm{MeV/c^2}$
  We choose about 3σ width for the mass distribution. The PDG value of η is $547.75\ \mathrm{MeV/c^2}$. The mass distributions are shown in [Fig 2.15(b)] and [Fig 2.16(b)].

- Mass Fit:
  The decay of $\eta \to \gamma\gamma$ is neutral mode decay. Therefore, we constrain the fit of η by the PDG value of η, $547.862\ \mathrm{MeV/c^2}$. We require the confidence level should be greater than 0 to reject the events which fail the fit of mass fit. After the fitting, the mass distribution of η are shown in [Fig 2.15(a)][Fig 2.16 (a)].

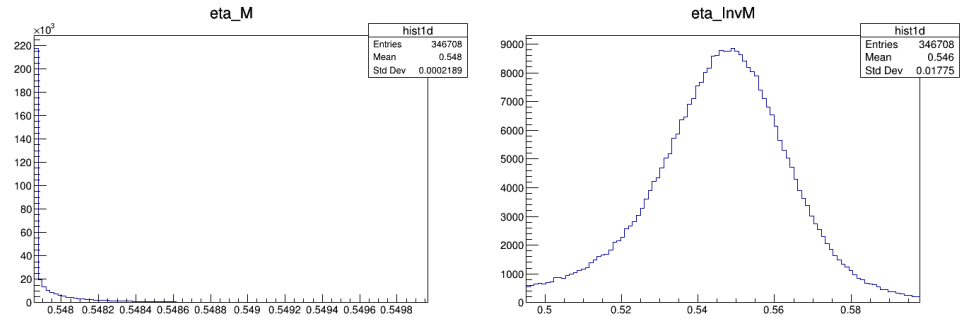

(a) eta_M (left) : The M_η distribution performed by vertex fitting.

(b) eta_InvM (right) : The M_η distribution determined by adding 4-momentum vectors of particle's daughter.

Fig 2.15 The M_η of the decay channel $J/\psi \to e^+e^-(\gamma), \eta \to \gamma\gamma$

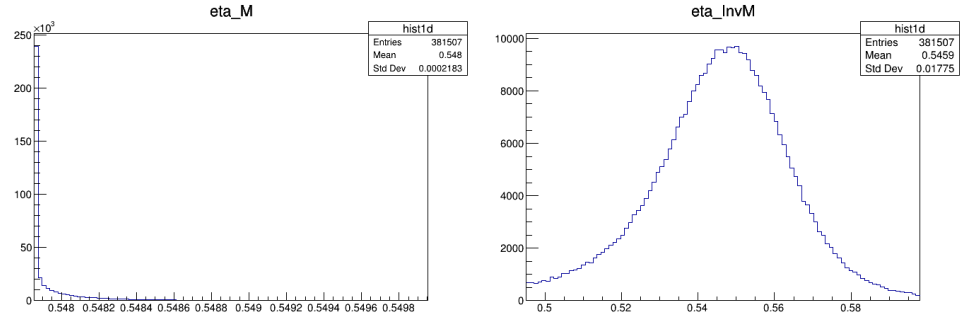

(a) eta_M (left) : The M_η distribution performed by vertex fitting.

(b) eta_InvM (right) : The M_η distribution determined by adding 4-momentum vectors of particle's daughter.

Fig 2.16 The M_η of the decay channel $J/\psi \to \mu^+\mu^-, \eta \to \gamma\gamma$

For the decay mode $\eta \to \pi^+\pi^-\pi^0$, the selections are as follows.

- Particle Identification:
  For the π^+ and π^- candidates, we require the particle identification probability $\frac{\mathcal{L}_\pi}{(\mathcal{L}_e+\mathcal{L}_\mu+\mathcal{L}_\pi+\mathcal{L}_K+\mathcal{L}_p+\mathcal{L}_d)} > 0.5$.
  For the π^0 candidates, the selections are as follows.

  - Gamma Energy:
    The energy $E_\gamma > 100$ MeV.

  - Mass window of π^0: $114\ \mathrm{MeV/c^2} < M_{\pi^0} < 160\ \mathrm{MeV/c^2}$
    We choose about 3σ width for the mass distribution. The PDG value of π^0 is $134.977\ \mathrm{MeV/c^2}$. The mass distributions are shown in [Fig 2.19(b)] and [Fig 2.20(b)].

  - Mass Fit:
    The decay of $\pi^0 \to \gamma\gamma$ is a neutral mode decay. We use the massKFitter to fit the particle with the constrain of mass with the PDG Value $134.977\ \mathrm{MeV/c^2}$. We require the confidence level should be greater than 0 to reject the events which fail the fit of mass fit. After the fitting, the mass distribution of π^0 are shown in [Fig 2.19 (a)][Fig 2.20 (a)].

- Mass window: $537\ \mathrm{MeV/c^2} < M_\eta < 559\ \mathrm{MeV/c^2}$
  We choose about 3σ width for the mass distribution. The PDG value of η is $547.862.\ \mathrm{MeV/c^2}$. The mass distributions are shown in [Fig 2.17 (b)] and [Fig 2.18(b)].

- Momentum constraint:
  We request the momenta (p) of each daughter of η should be p $>$ 200 MeV/c.

- Mass Fit and Vertex Fit.
  Vertex Fit: The $\pi^+\pi^-$ of η can be constrained with the charge tracks. The fitting technique is to obtain the vertices which is based on the least square method using the Lagrange multiplier method. [13]

  Mass Fit : The mass of η in PDG value is 547.862. MeV/c^2. The Kfitter of Mass Fit is using invariant mass of η and the reoncstructed $\pi^+\pi^-\pi^0$ to do the fitting.
  We require the confidence level should be greater than 0 to reject the events which fail the fit of mass fit and vertex fit.
  After the fitting, the mass distribution of η are shown in [Fig 2.17(a)][Fig 2.18(a)].

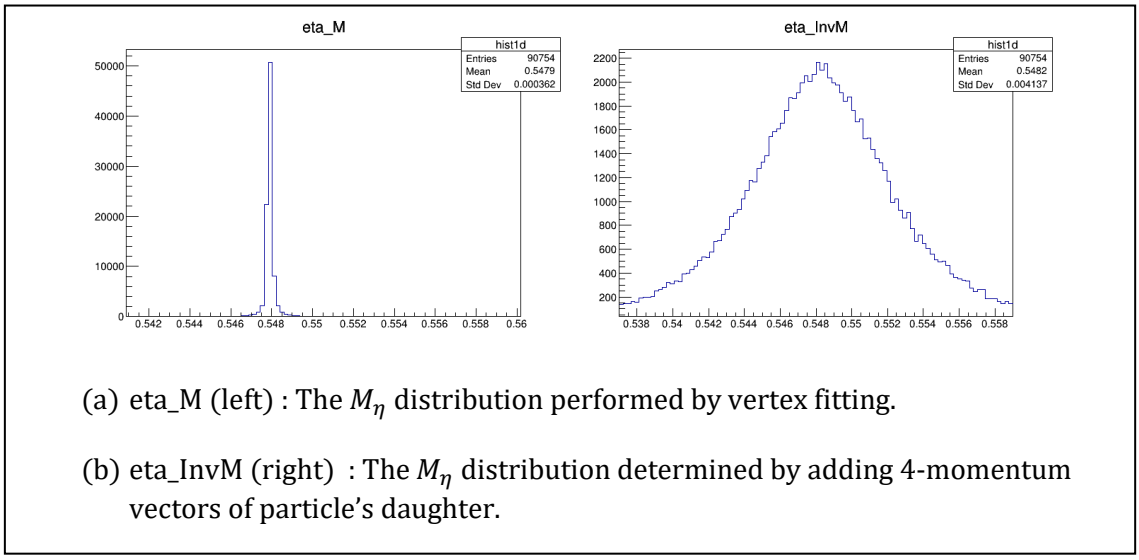

(a) eta_M (left) : The M_η distribution performed by vertex fitting.

(b) eta_InvM (right) : The M_η distribution determined by adding 4-momentum vectors of particle's daughter.

Fig 2.17 The M_η of the decay channel $J/\psi \to e^+e^-(\gamma), \eta \to \pi^+\pi^-\pi^0$

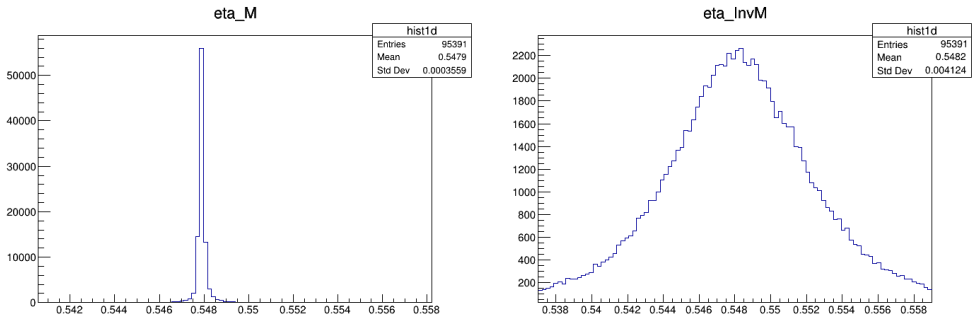

(a) eta_M (left) : The M_η distribution performed by vertex fitting.

(b) eta_InvM (right) : The M_η distribution determined by adding 4-momentum vectors of particle's daughter.

Fig 2.18 The M_η of the decay channel $J/\psi \to \mu^+\mu^-, \eta \to \pi^+\pi^-\pi^0$

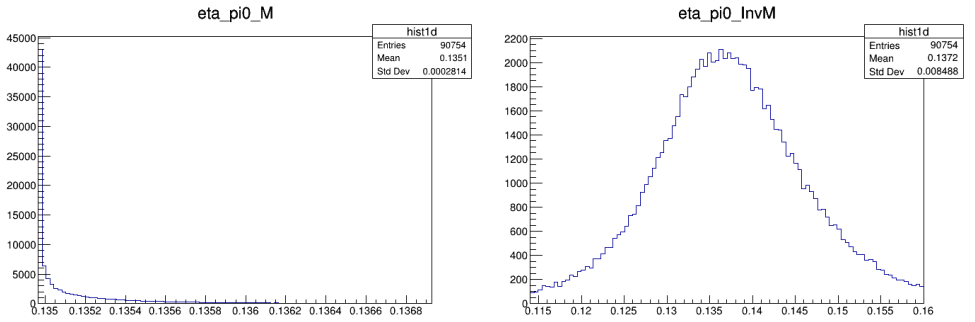

(a) eta_pi0_M (left) : The M_{π^0} distribution performed by vertex fitting.

(b) eta__pi0_InvM (right) : The M_{π^0} distribution determined by adding 4-momentum vectors of particle's daughter.

Fig 2.19 The M_{π^0} of the decay channel $J/\psi \to e^+e^-(\gamma), \eta \to \pi^+\pi^-\pi^0$

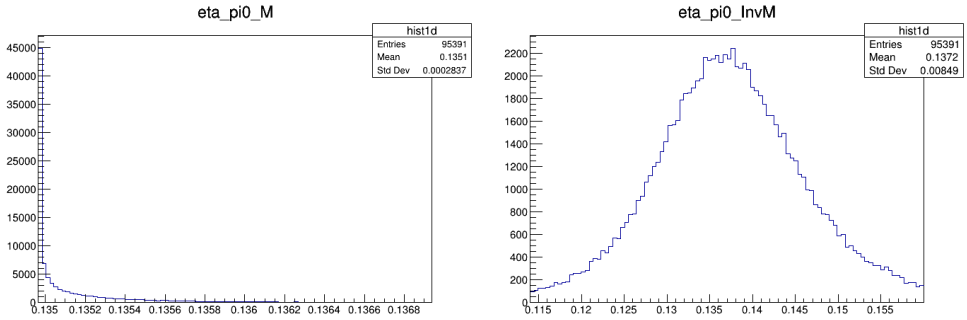

(a) eta_pi0_M (left) : The M_{π^0} distribution performed by vertex fitting.

(b) eta__pi0_InvM (right) : The M_{π^0} distribution determined by adding 4-momentum vectors of particle's daughter.

Fig 2.20 The M_{π^0} of the decay channel $J/\psi \to \mu^+\mu^-, \eta \to \pi^+\pi^-\pi^0$

2.3.5 Requirements for reconstructed B^0

The selected candidates of J/ψ and η can be reconstructed as B^0. We use two variables to improve the selections of our B^0 candidates.

The used two variables are beam constrained mass (M_{bc}) and energy difference (ΔE). They are as follows.

- Beam Constrained Mass: $M_{bc} = \sqrt{\left(E^{*2}_{beam} - \Sigma P_i^2\right)}$.

- Energy Difference: $\Delta E = \Sigma E_i - E^*_{beam}$.

E^*_{beam} is the energy of center of mass, E_i are the energy of the candidate of particle decayed from B^0, and P_i are the three-momenta of the candidate of particle decayed from B^0. In order to reduce background events in the beginning, we require these two variables $5.2\ \mathrm{GeV/c^2} < M_{bc} < 5.3\ \mathrm{GeV/c^2}$ and $-0.2\ GeV < \Delta E < 0.2\ GeV$.

For the $\eta \to \gamma\gamma$ mode, the variables range of signal yields that we require are as follows:

- $-0.1\ GeV < \Delta E < 0.05\ GeV$

- $5.27\ \mathrm{GeV/c^2} < M_{bc} < 5.29\ \mathrm{GeV/c^2}$

For the $\eta \to \pi^+\pi^-\pi^0$ mode, the variables range of signal yields that we require are as follows:

- $-0.05\ GeV < \Delta E < 0.05\ GeV$

- $5.27\,\mathrm{GeV/c^2} < M_{bc} < 5.29\,\mathrm{GeV/c^2}$

The ΔE and M_{bc} distributions are shown as Fig 2.21, Fig 2.22, Fig 2.23 and Fig 2.24.

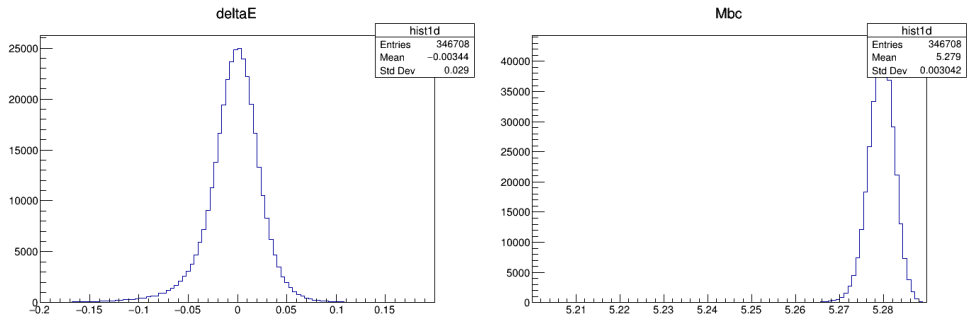

(a) deltaE (left) : The ΔE distribution

(b) Mbc (right) : The M_{bc} distribution

Fig 2.21 ΔE and M_{bc} distributions of decay mode $J/\psi \to e^+e^-(\gamma), \eta \to \gamma\gamma$

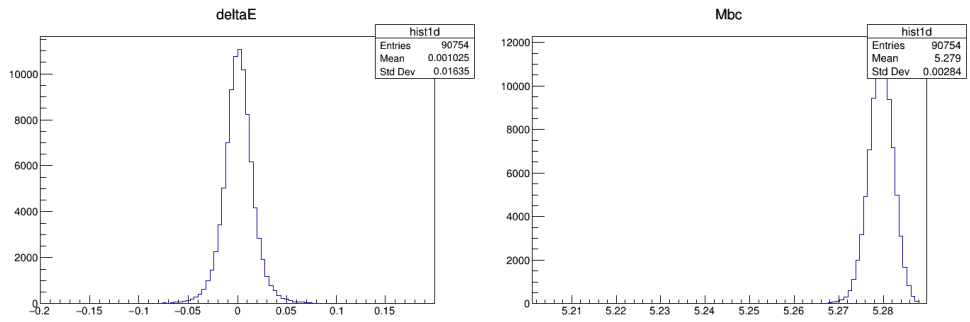

(a) deltaE (left) : The ΔE distribution

(b) Mbc (right) : The M_{bc} distribution

Fig 2.22 ΔE and M_{bc} distributions of decay mode $J/\psi \to e^+e^-(\gamma), \eta \to \pi^+\pi^-\pi^0$

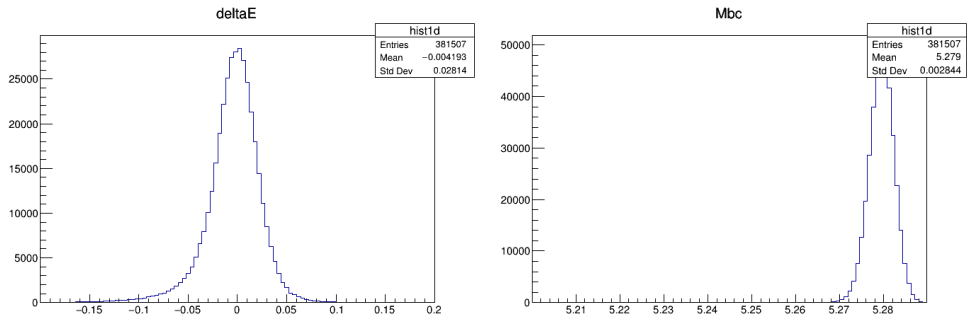

(a) deltaE (left) : The ΔE distribution

(b) Mbc (right) : The M_{bc} distribution

Fig 2.23 ΔE and M_{bc} distributions of decay mode $J/\psi \to \mu^+\mu^-, \eta \to \gamma\gamma$

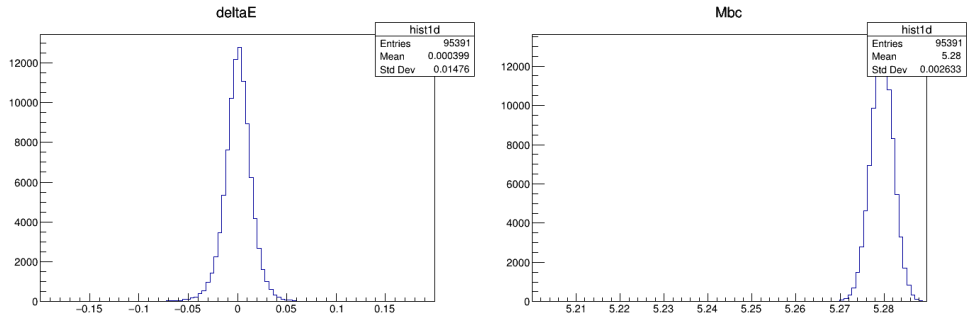

(a) deltaE (left) : The ΔE distribution

(b) Mbc (right) : The M_{bc} distribution

Fig 2.24 ΔE and M_{bc} distributions of decay mode $J/\psi \to \mu^+\mu^-, \eta \to \pi^+\pi^-\pi^0$

2.3.6 Signal PDF

We simulate 2 million events for signal Monte Carlo simulation in each mode. For the signal probability density functions (PDF) of ΔE, we use Crystal Ball Shape and Gaussian Function to do the fitting. Because the number of events in the signal yield region of $J/\psi \to e^+e^-(\gamma), \eta \to \pi^+\pi^-\pi^0$ and $J/\psi \to \mu^+\mu^-, \eta \to \pi^+\pi^-\pi^0$ are not enough to do the better fitting during our Toy & Pull Test separately Therefore, we combine the events of $J/\psi \to l^+l^-$ ($l = e\ or\ \mu$), $\eta \to \pi^+\pi^-\pi^0$ while doing the ΔE distribution fitting of signal PDF, as well as the events of $J/\psi \to l^+l^-$ ($l = e\ or\ \mu$), $\eta \to \gamma\gamma$.

We combine one Crystal Ball Shape function and two Gaussian functions in one PDF to fit the ΔE distribution of signal PDF. The results are shown as Fig 2.25 and Fig 2.26.

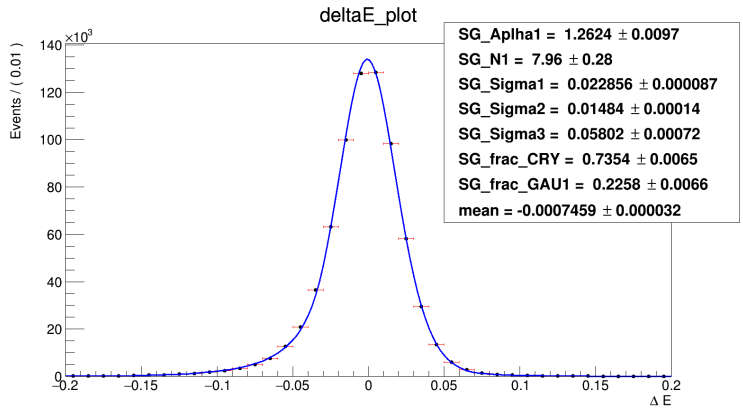

Fig 2.25 The signal PDF of ΔE distribution in the decay mode $J/\psi \to l^+l^-, \eta \to \gamma\gamma$

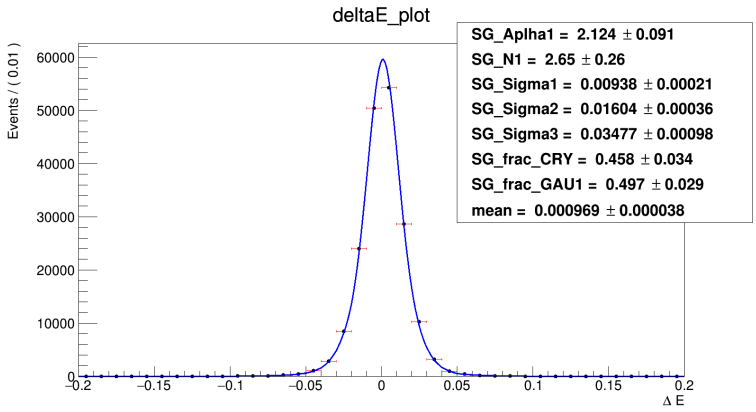

Fig 2.26 The signal PDF of ΔE distribution in the decay mode $J/\psi \to l^+l^-, \eta \to \pi^+\pi^-\pi^0$

Chapter 3 Background

3.1 Background Survey

3.1.1 Background Monte Carlo Event Type

There are 6 kinds of backgrounds we need to study, $q\bar{q}$ ($q = u, d, c, s$), mixed, and charged. The number of generated events for the backgrounds are listed in Table 3.1. Each batch of integrated luminosity is $100fb^{-1}$. We use 8 batches of the generated backgrounds in MC13 .

Sample	Number of events ($\times 10^6$)	Number of total events of 8 batches ($\times 10^6$)
mixed	51	408
charged	54	432
uubar	160.5	1284
ddbar	40.1	320.8
ssbar	38.3	306.4
ccbar	132.9	1063.2

Table 3.1 The number of generated events in the thirteenth official background Monte Carlo campaign (MC13)

3.1.2 $R2$ Definition

In the beginning, we want to use R2 cut to reduce the $q\bar{q}$ backgrounds. The R2 definition is as follows.

Fox-Wolfram moments are an established tool to analyze geometric patterns in QCD. The Fox-Wolfram moments $H_l, l = 0, 1, 2 \ldots$ are defined by

$$H_l = \sum_{i,j} \frac{(|P_i||P_j|)}{E_j^{vis}} P_l(\cos\theta_{ij})$$

where θ_{ij} is the opening angle between charged tracks or photons of i and j, E_{vis} is the total visible energy of the event, P_l are the Legendre polynomials and $|P_i|$ and $|P_j|$ are the momenta of the charged tracks or photons. R_2 is defined as $\frac{H_2}{H_0}$. [14]

We want to use the R2 to do the 3D fitting. However, while doing the 3D fitting, the functions cannot fit well in R2 side. We do not use the R2 variable.

3.1.3 Backgrounds

We want to understand the main backgrounds in our analysis, and use the variable, "mcPDG", to get the information of the particle ID in MC. The main backgrounds are listed in Table 3.2, Table 3.3, Table 3.4 and Table 3.5.

$B^0 \to J/\psi(e^+e^-(\gamma))\eta(\gamma\gamma)$	
Background Components	Number of events
$J/\psi\Upsilon(4S)$	30
Z^0Z^0	5
$Z^0\eta$	2
$Z^0\omega$	2
$\Upsilon(4S)\Upsilon(4S)$	1
$B_0\Upsilon(4S)$	1

Table 3.2 The main components of backgrounds in $B^0 \to J/\psi(e^+e^-(\gamma))\eta(\gamma\gamma)$ mode.

$B^0 \to J/\psi(e^+e^-(\gamma))\eta(\pi^+\pi^-\pi^0)$	
Background Components	Number of events
$J/\psi\Upsilon(4S)$	8
Z^0Z^0	1

Table 3.3 The main components of backgrounds in $B^0 \to J/\psi(e^+e^-(\gamma))\eta(\pi^+\pi^-\pi^0)$ mode.

$B^0 \to J/\psi(\mu^+\mu^-)\eta(\gamma\gamma)$	
Background Components	Number of events
$\boldsymbol{J/\psi\Upsilon(4S)}$	42
$\boldsymbol{Z^0Z^0}$	15
$\boldsymbol{Z^0\eta}$	3
$\boldsymbol{\Upsilon(4S)\eta}$	1
$J/\psi B^0$	1
$J/\psi K_S^0$	1

Table 3.4 The main components of backgrounds in $B^0 \to J/\psi(\mu^+\mu^-)\eta(\gamma\gamma)$ mode.

$\boldsymbol{B^0 \to J/\psi(\mu^+\mu^-)\eta(\pi^+\pi^-\pi^0)}$	
Background Components	Number of events
$\boldsymbol{J/\psi\Upsilon(4S)}$	12
$\boldsymbol{Z^0\eta}$	2
$\boldsymbol{Z^0\eta'}$	1
$\boldsymbol{Z^0Z^0}$	1
$\boldsymbol{Z^0D^-}$	1

Table 3.5 The main components of backgrounds in $B^0 \to J/\psi(\mu^+\mu^-)\eta(\pi^+\pi^-\pi^0)$ mode.

3.2 Background PDF

For the background events introduced in Chapter 3.1.3, the ΔE distribution shape of these events are fitted as background PDFs. The background PDFs are fitted by 2nd order Chebyshev Polynomial function. The results are shown as Fig 3.1, Fig 3.2, Fig 3.3 and Fig 3.4.

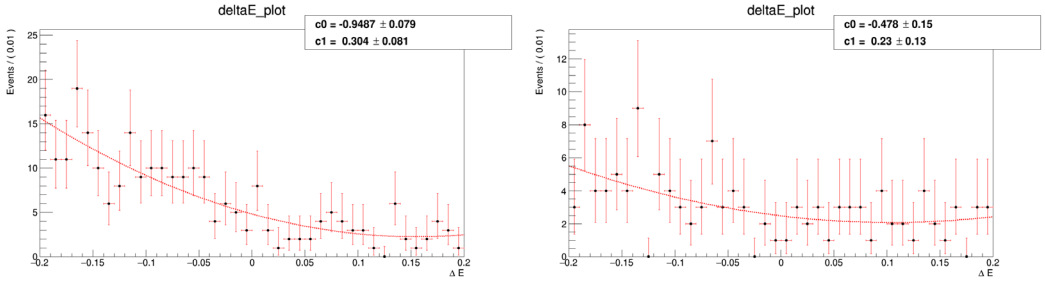

(a) deltaE (left) : The background PDF of ΔE distribution in $b\bar{b}$ backgrounds.

(b) deltaE (right) : The background PDF of ΔE distribution in $q\bar{q}$ backgrounds.

Fig 3.1 The background PDFs of ΔE distribution in decay channel $J/\psi \to l^+l^-, \eta \to \gamma\gamma$

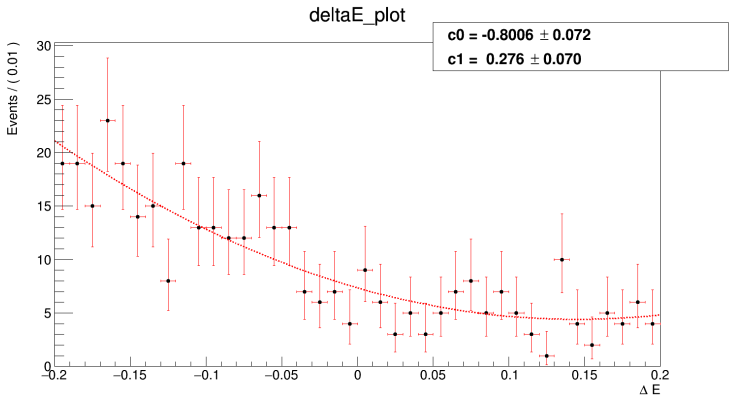

Fig 3.2 The background PDF of ΔE distribution combined $q\bar{q}$ and $b\bar{b}$ for decay channel $J/\psi \to l^+l^-, \eta \to \gamma\gamma$

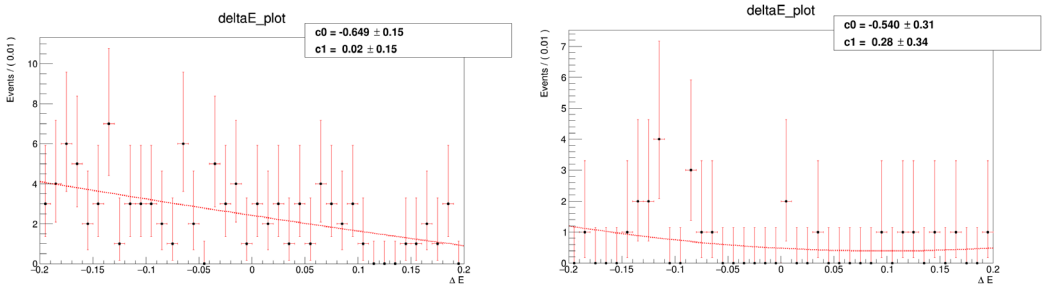

(a) deltaE (left) : The background PDF of ΔE distribution in $b\bar{b}$ backgrounds.

(b) deltaE (right) : The background PDF of ΔE distribution in $q\bar{q}$ backgrounds.

Fig 3.3 The background PDFs of ΔE distribution in decay channel $J/\psi \to l^+l^-, \eta \to \pi^+\pi^-\pi^0$

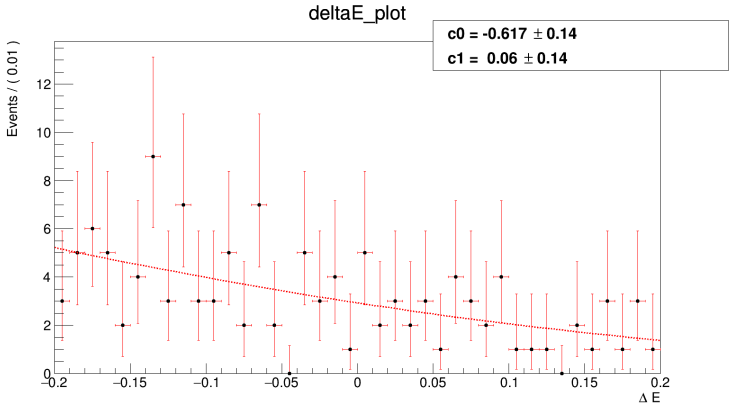

Fig 3.4 The background PDF of ΔE combined $q\bar{q}$ and $b\bar{b}$ for decay channel $J/\psi \to l^+l^-, \eta \to \pi^+\pi^-\pi^0$

3.3 Control Sample

The Signal MC is not perfect. We use the control sample to study the difference between the Signal MC and real data. We get the fitting shifts between the Signal MC of Control Sample and real data to fix the PDF of Signal MC.

We select $B^{\pm} \to J/\psi\ K^{*\pm}(892), (J/\psi \to l^{+}l^{-})\ (K^{*\pm} \to\ K^{\pm}\pi^{0})$ as our control sample. [15]

The event selections of our control sample are as follows:

- J/ψ : The selection is same as our decay mode's.
- π^{0} : The selection is same as our decay mode's.
- $K^{\pm}, \pi^{\pm}$: "good" selection in Belle II stdK module.
- The particle identification probability of $K^{\pm}, \pi^{\pm}$ with the selection "good" $\frac{\mathcal{L}_{\pi}}{(\mathcal{L}_{e}+\mathcal{L}_{\mu}+\mathcal{L}_{\pi}+\mathcal{L}_{K}+\mathcal{L}_{p}+\mathcal{L}_{d})} > 0.1$
- $K^{*\pm}$: Mass Constraint : $0.79\ GeV/c^{2} < M_{K^{*\pm}} <\ 0.99\ GeV/c^{2}$
- B^{+} Constraint: $5.2\ GeV/c^{2} <\ M_{bc} < 5.3\ GeV/c^{2},\ -0.2\ GeV < \Delta E < 0.2\ GeV$

For the signal MC of control sample, we use two million of $B \to J/\psi(l^{+}l^{-})K^{*+}$ events.

We use the same function of Signal PDF to fit the control sample. The result is shown as Fig 3.5.

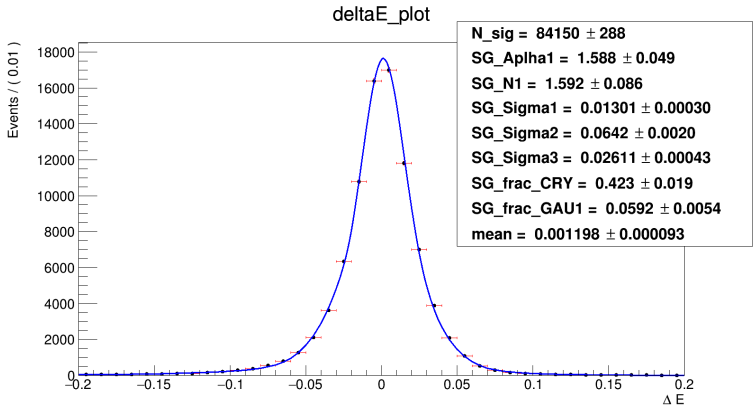

Fig 3.5 The signal PDF of ΔE distribution in control sample $B^{\pm} \to J/\psi\, K^{*\pm}(892), (J/\psi \to l^{+}l^{-})\ (K^{*\pm} \to K^{\pm}\pi^{0})$

For the current Belle II Data, 39.6551 fb^{-1}[Appendix B], the number of data events are used for this control sample.

The result is shown in the Fig 3.6. Due to the few number of events in Belle II Data, the fitting error will be to large. We use the full data of Belle experiment to do our fitting again. The fitting result is shown in Fig 3.7.

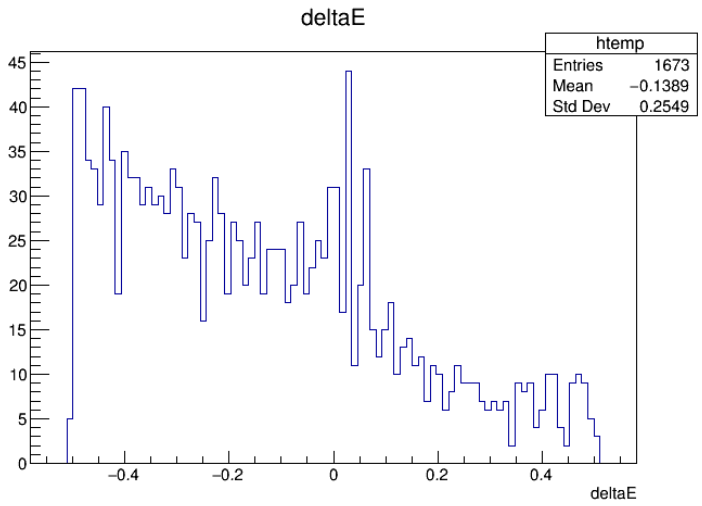

Fig 3.6 ΔE distribution of control sample $B^{\pm} \to J/\psi\, K^{*\pm}(892), (J/\psi \to l^{+}l^{-})\ (K^{*\pm} \to K^{\pm}\pi^{0})$ use Belle II Data.

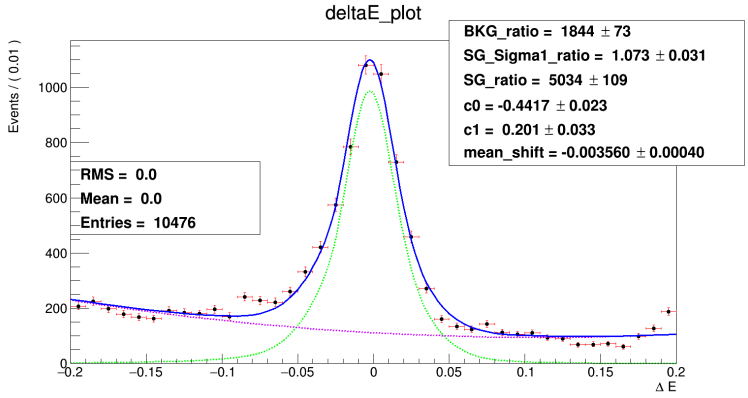

Fig 3.7 ΔE distribution of control sample $B^{\pm} \to J/\psi\, K^{*\pm}(892), (J/\psi \to l^{+}l^{-})\ (K^{*\pm} \to K^{\pm}\pi^{0})$ use Belle Data.

In the Fig 3.7, we get the mean shift between the signal Monte Carlo and the Belle data. The mean shift is the mean value of ΔE in data subtract the mean value of ΔE in MC. The widen ration is the width of ΔE in data divide the width of ΔE in MC. The results are shown Table 3.6.

Mean Shift (GeV)	Widen Ratio
-0.003560	1.073

Table 3.6 The mean shift and the widen ratio of the signal PDF in control sample.

3.4 Toy MC & PULL Test

For avoiding the bias of PDF which is combined with signal PDF and background PDF. We use toy test and PULL Test to check it. The PULL distribution is defined as

$$PULL = \frac{FitNumber - InputNumber}{FitError}$$

- InputNumber: The input number of event in MC ensemble sample.

- FitNumber: The point in the Poisson function.

- FitError: the width of the Poisson function (the point in Poisson to the mean value of the Poisson function).

If the mean of PULL is close to 0 and the sigma of PULL is close to 1, it means that PDF will not cause the spike.

To calculate the PULL TEST, we need to get the number of signal and background in the signal yield region.

The number of signal in the signal yield region is calculated as following equation and the result is shown as Table 3.7.

	N_s	$N_{B\bar{B}}$	ϵ	$Br(B^0 \to J/\psi)$	$Br(J/\psi \to)$	$Br(\eta \to)$
$J/\psi \to e^+e^-$ $\eta \to \gamma\gamma$	36.1844		16.755%		6.851%	39.41%
$J/\psi \to e^+e^-$ $\eta \to \pi^+\pi^-\pi^0$	5.6180		4.473%		6.851%	22.92%
$J/\psi \to \mu^+\mu^-$ $\eta \to \gamma\gamma$	36.3708	$= 771 \times 10^6$	18.593%	$\times 1.08 \times 10^{-5}$	5.961%	39.41%
$J/\psi \to \mu^+\mu^-$ $\eta \to \pi^+\pi^-\pi^0$	5.3834		4.732%		5.961%	22.92%

Table 3.7 The number of signals in the signal yield region.

The number of backgrounds N_{bkg} in $\eta \to \gamma\gamma$ decay are calculated by the following equation. The A_3, A_2, A_1 are the number of events in $0.2\ GeV > \Delta E > 0.05 GeV$, $0.05\ GeV > \Delta E > -0.1\ GeV$ and $-0.1\ GeV > \Delta E > -0.2\ GeV$, respectively. All of them are in the $5.2\ \mathrm{GeV/c^2} < M_{bc} < 5.26\ \mathrm{GeV/c^2}$. The B_3 and B_1 are the number of events in $0.2\ GeV > \Delta E > 0.05 GeV$ and $-0.1\ GeV > \Delta E > -0.2\ GeV$, respectively. Both of them are in the $5.27\ \mathrm{GeV/c^2} < M_{bc} < 5.29\ \mathrm{GeV/c^2}$. In this calculation, we assume the background distribution in $5.2\ \mathrm{GeV/c^2} < M_{bc} < 5.26\,\mathrm{GeV/c^2}$ is linearly, same as $5.27\ \mathrm{GeV/c^2} < M_{bc} < 5.29\ \mathrm{GeV/c^2}$.

The number of backgrounds N_{bkg} in $\eta \to \pi^+\pi^-\pi^0$ decay are calculated by the following equation. The A_3, A_2, A_1 are the number of events in $0.2\ GeV > \Delta E > 0.05 GeV$, $0.05\ GeV > \Delta E > -0.05\ GeV$ and $-0.05\ GeV > \Delta E > -0.2\ GeV$, respectively. All of them are in the $5.2\ \mathrm{GeV/c^2} < M_{bc} < 5.26\ \mathrm{GeV/c^2}$. The B_3 and B_1 are the number of

events in $0.2\ GeV > \Delta E > 0.05 GeV$ and $-0.05\ GeV > \Delta E > -0.2\ GeV$, respectively. Both of them are in the $5.27\ \mathrm{GeV/c^2} < M_{bc} < 5.29\ \mathrm{GeV/c^2}$. In this calculation, we assume the background distribution in $5.2\ \mathrm{GeV/c^2} < M_{bc} < 5.26\ \mathrm{GeV/c^2}$ is linearly, same as $5.27\ \mathrm{GeV/c^2} < M_{bc} < 5.29\ \mathrm{GeV/c^2}$.

$$N_{bkg} = A_2 \times \frac{(B_1 + B_3)}{A_1 + A_3}$$

The concept of calculating the number of background events is shown in Fig 3.8. The details are shown in Table 3.8, Table 3.9, Table 3.10 and Table 3.11.

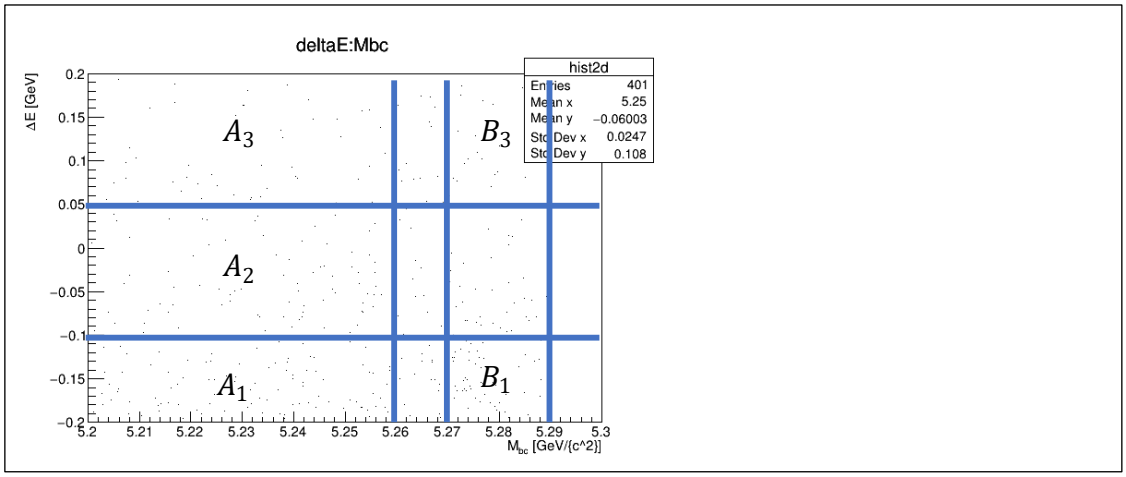

Fig 3.8 The concept of calculating the number of backgrounds event in the signal yield region.

Background Type	N_{bkg}	A_1	A_2	A_3	B_1	B_3
$b\bar{b}$	68.80	104	83	48	104	22
u, d, s	9.26	34	33	23	13	3
$c\bar{c}$	13.67	32	41	37	17	6
Total	81.53					

Table 3.8 The details of background number in the signal yield estimation for the decay $J/\psi \rightarrow e^+e^-(\gamma), \eta \rightarrow \gamma\gamma$

Background Type	N_{bkg}	A_1	A_2	A_3	B_1	B_3
$b\bar{b}$	73.32	137	95	47	123	19
u, d, s	28.99	84	83	62	39	12
$c\bar{c}$	27.74	62	60	31	29	14
Total	115.58					

Table 3.9 The details of background number in the signal yield estimation for the decay $J/\psi \rightarrow e^+e^-(\gamma), \eta \rightarrow \pi^+\pi^-\pi^0$

Background Type	N_{bkg}	A_1	A_2	A_3	B_1	B_3
$b\bar{b}$	10.38	764	22	25	29	13
u, d, s	0.09	4	1	7	0	1
$c\bar{c}$	1.65	12	7	5	3	1
Total	10.77					

Table 3.10 The details of background number in the signal yield estimation for the decay $J/\psi \rightarrow \mu^+\mu^-, \eta \rightarrow \gamma\gamma$

Background Type	N_{bkg}	A_1	A_2	A_3	B_1	B_3
$b\bar{b}$	9.44	61	15	28	47	9
u, d, s	1.64	15	4	7	7	2
$c\bar{c}$	4.85	19	16	14	8	2
Total	14.15					

Table 3.11 The details of background number in the signal yield estimation for the decay $J/\psi \to \mu^+\mu^-, \eta \to \pi^+\pi^-\pi^0$

The number of toy MC events is decided by the total number of signal and background events in the signal yield region. We generate them randomly according to Poisson distribution. The toy test results are shown in Fig 3.9 and Fig 3.11. The PULL test results are shown in Fig 3.10 and Fig 3.12. The details of PULL test are listed in Table 3.12.

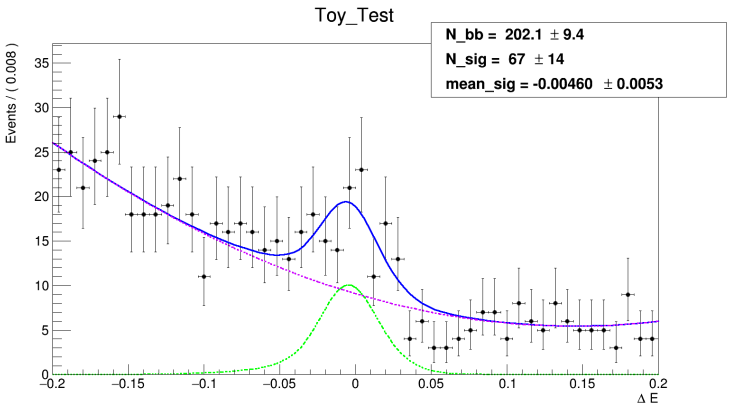

Fig 3.9 The toy test fitting plot of the $\eta \to \gamma\gamma$ decay mode.

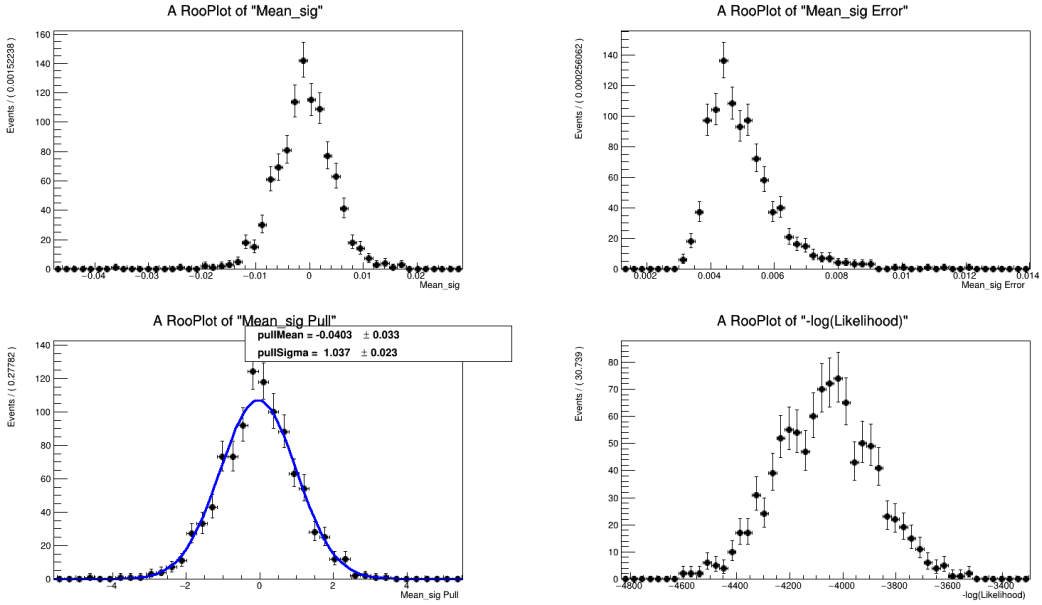

Fig 3.10 The PULL Test of the $\eta \to \gamma\gamma$ decay mode.

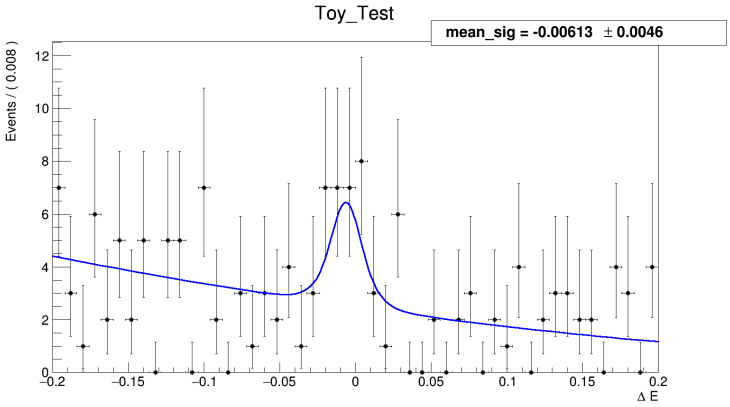

Fig 3.11 The toy test fitting plot of the $\eta \to \pi^+\pi^-\pi^0$ decay mode.

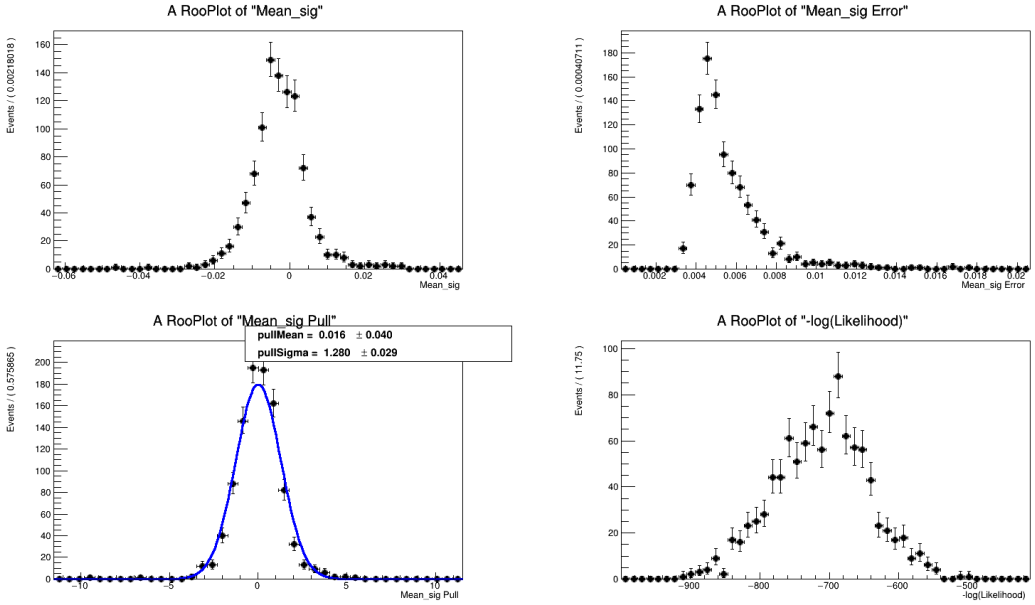

Fig 3.12 The PULL Test of the $\eta \to \pi^+\pi^-\pi^0$ decay mode.

Decay	PULL Mean	PULL Sigma
$B^0 \to J/\psi\eta(\eta \to \gamma\gamma)$	-0.040 ± 0.033	1.037 ± 0.023
$B^0 \to J/\psi\eta(\eta \to \pi^+\pi^-\pi^0)$	0.016 ± 0.040	1.280 ± 0.029

Table 3.12 The mean and sigma of PULL test.

Chapter 4 Systematic Errors

4.1 Official Systematic Errors

4.1.1 Tracking

For the charged track, which $P_t > 200$ MeV/c, the systematic uncertainty for experiment from 7 to 71 that we measured is $(-0.13 \pm 0.30 \pm 0.10)\%$. So, we apply the systematic uncertainty of $\mathbf{0.35}\%$ per track. [16]

4.1.2 Number of $B\bar{B}$ events

There are $(771.581 \pm 10.566) \times 10^6$ $B\bar{B}$ events in the Belle Full Data, so the error from the number of $B\bar{B}$ events is 1.37%. The details of event amounts and the statistical errors can be found on the Belle Internal Web Page. [17]

4.1.3 KID selection

For the pion and kaon, we need to correct the reconstructed efficiency in data. We use the final KID table to do the correction [18]. The result of our correction is listed as Table 4.1.

		SVD1	SVD2
π^+	Data	0.8893 ± 0.0053	0.8859 ± 0.0056
	Correction for signal efficiency	0.8864	
	Systematic error	0.63%	
π^-	Data	0.9004 ± 0.0054	0.8916 ± 0.0058
	Correction for signal efficiency	0.8930	
	Systematic error	0.64%	

Table 4.1 The Correction of the efficiency and the systematic error from KID

- π^+ KID efficiency correction. There are 18 events in SVD1 data and 110 events in SVD2 data.

$$\left(\frac{18}{18+110}\right) \times (0.8893) + \left(\frac{110}{18+110}\right) \times (0.8859) = 0.8864$$

- π^+ KID systematic error. There are 18 events in SVD1 data and 110 events in SVD2 data.

$$\left(\frac{18}{18+110}\right) \times \left(\frac{0.0053}{0.8893}\right) + \left(\frac{110}{18+110}\right) \times \left(\frac{0.0056}{0.8859}\right) = 0.0063$$

- π^- KID efficiency correction. There are 16 events in SVD1 data and 86 events in SVD2 data.

$$\left(\frac{16}{16+86}\right) \times (0.9004) + \left(\frac{86}{16+86}\right) \times (0.8916) = 0.8930$$

- π^- KID systematic error. There are 16 events in SVD1 data and 86 events in SVD2 data.

$$\left(\frac{16}{16+86}\right) \times \left(\frac{0.0054}{0.9004}\right) + \left(\frac{86}{16+86}\right) \times \left(\frac{0.0058}{0.8916}\right) = 0.0064$$

4.1.4 Lepton selection

In our decay mode, the leptons are muon and electron. The selection variables of the lepton identification are "Muon ID" for muon and "Electron ID" for electron. The systematic errors and correction are calculated by the PIDJOINT group in Belle. The result of the systematic errors and the correction are list as Table 4.4, Table 4.5, Table 4.6 and Table 4.7.

For the reconstructed efficiency correction of electron, there are two efficiency tables shown as Table 4.2.

	Experiment	Efficiency Table
$e1$	Exp 7 - 27	eid_data-mc_corr_svd1.dat
$e2$	Exp 31 - 73	eid_data-mc_corr_exp31-65-caseB.dat

Table 4.2 The lepton ID for $e^{\pm}$ correction file related to the experiment number of Belle data.

For the reconstructed efficiency correction of muon, there are four efficiency tables shown as Table 4.3.

	Experiment	Efficiency Table
$mu1$	exp7-27	muid_data-mc_corr_svd1.dat
$mu2$	exp31-39 and exp45a (run1-220)	muid_data-mc_corr_exp31-39-45a-caseB.dat
$mu3$	exp41-49 except exp45a (run1-220)	muid_data-mc_corr_exp41-49-caseB.dat
$mu4$	exp51-73	muid_data-mc_corr_exp51-65-caseB.dat

Table 4.3 The lepton ID for $\mu^{\pm}$ correction file related to the experiment number of Belle data.

	Event Tracks Amount	Correction	
e^+	4	0.9787 ± 0.0190	$e1$
	376	0.9806 ± 0.0142	$e2$
correction		0.9806	
Systematic error		1.45%	

Table 4.4 The efficiency correction and the systematic error for e^+.

- e^+ Lepton ID efficiency correction. There are 4 tracks in e1 and 376 tracks in e2. The details of e1 and e2 are shown in Table 4.2.

$$\left(\frac{4}{4+376}\right) \times (0.9787) + \left(\frac{376}{4+376}\right) \times (0.9806) = 0.9806$$

- e^+ Lepton ID systematic error. There are 4 tracks in e1 and 376 tracks in e2. The details of e1 and e2 are shown in Table 4.2.

$$\left(\frac{4}{4+376}\right) \times \left(\frac{0.0190}{0.9787}\right) + \left(\frac{376}{4+376}\right) \times \left(\frac{0.0142}{0.9806}\right) = 0.0145$$

	Event Tracks Amount	Correction	
e^-	20	0.9803 ± 0.0166	$e1$
	316	0.9801 ± 0.0142	$e2$
correction		0.9801	
Systematic error		1.46%	

Table 4.5 The efficiency correction and the systematic error for e^-.

- e^- Lepton ID efficiency correction. There are 20 tracks in e1 and 316 tracks in e2. The details of e1 and e2 are shown in Table 4.2.

$$\left(\frac{20}{20+316}\right)\times(0.9803)+\left(\frac{316}{20+316}\right)\times(0.9801)=0.9801$$

- e^- Lepton ID systematic error . There are 20 tracks in e1 and 316 tracks in e2. The details of e1 and e2 are shown in Table 4.2.

$$\left(\frac{20}{20+316}\right)\times\left(\frac{0.0166}{0.9803}\right)+\left(\frac{20}{20+316}\right)\times\left(\frac{0.0142}{0.9801}\right)=0.0146$$

	Event Tracks Amount	Correction	
μ^+	12	0.9927 ± 0.0282	$mu1$
	4	0.9494 ± 0.0096	$mu2$
	0	0	$mu3$
	640	0.9578 ± 0.0193	$mu4$
correction		0.9584	
Systematic error		2.02%	

Table 4.6 The efficiency correction and the systematic error for μ^+.

- μ^+ Lepton ID efficiency correction. The are 12 tracks in mu1, 4 tracks in mu2, 0 track in mu3 and 640 tracks in mu4. The details of mu1. mu2, mu3 and mu4 are shown in Table 4.3.

$$\begin{aligned}&\left(\frac{12}{12+4+0+640}\right)\times(0.9927)\\&+\left(\frac{4}{12+4+0+640}\right)\times(0.9494)\\&+\left(\frac{0}{12+4+0+640}\right)\times(0)\\&+\left(\frac{640}{12+4+0+640}\right)\times(0.9578)=0.9584\end{aligned}$$

- μ^+ Lepton ID systematic error. The are 12 tracks in mu1, 4 tracks in mu2, 0 track in mu3 and 640 tracks in mu4. The details of mu1. mu2, mu3 and mu4 are shown in Table 4.3.

$$\left(\frac{12}{12+4+0+640}\right)\times\left(\frac{0.0282}{0.9927}\right) + \left(\frac{4}{12+4+0+640}\right)\times\left(\frac{0.0096}{0.9494}\right) + \left(\frac{0}{12+4+0+640}\right)\times(0) + \left(\frac{640}{12+4+0+640}\right)\times\left(\frac{0.0193}{0.9578}\right) = 0.0202$$

	Event Tracks Amount	Correction	
μ^-	16	0.9916 ± 0.0265	$mu1$
	6	0.8801 ± 0.0139	$mu2$
	2	0.9662 ± 0.0186	$mu3$
	766	0.9574 ± 0.0197	$mu4$
correction		0.9575	
Systematic error		2.07%	

Table 4.7 The efficiency correction and the systematic error for μ^-.

- μ^- Lepton ID efficiency correction. The are 16 tracks in mu1, 6 tracks in mu2, 2 tracks in mu3 and 766 tracks in mu4. The details of mu1. mu2, mu3 and mu4 are shown in Table 4.3.

$$\left(\frac{16}{16+6+2+766}\right)\times(0.9916) + \left(\frac{6}{16+6+2+766}\right)\times(0.8801) + \left(\frac{2}{16+6+2+766}\right)\times(0.9662) + \left(\frac{766}{16+6+2+766}\right)\times(0.9574) = 0.9575$$

- μ^- Lepton ID systematic error. The are 16 tracks in mu1, 6 tracks in mu2, 2 tracks in mu3 and 766 tracks in mu4. The details of mu1. mu2, mu3 and mu4 are shown in Table 4.3.

$$\left(\frac{16}{16+6+2+766}\right)\times\left(\frac{0.0265}{0.9916}\right) + \left(\frac{6}{16+6+2+766}\right)\times\left(\frac{0.0139}{0.8801}\right) + \left(\frac{2}{16+6+2+766}\right)\times\left(\frac{0.0186}{0.9662}\right) + \left(\frac{766}{16+6+2+766}\right)\times\left(\frac{0.0197}{0.9574}\right) = 0.0207$$

4.2 J/ψ selection

In our J/ψ selection, we ask the decay angle of $J/\psi \rightarrow l^+l^-$ between 0.3 and 2.8 to reduce the $q\bar{q}$ backgrounds. We use control sample $B^{\pm} \rightarrow J/\psi\ K^{*\pm}(892), (J/\psi \rightarrow l^+l^-)\ (K^{*\pm} \rightarrow K^{\pm}\pi^0)$ to calculate the systematic errors due to the selection of decay angle in our decay. The distributions and the fitting results are shown as Fig 4.1, Fig 4.2 and Table 4.8.

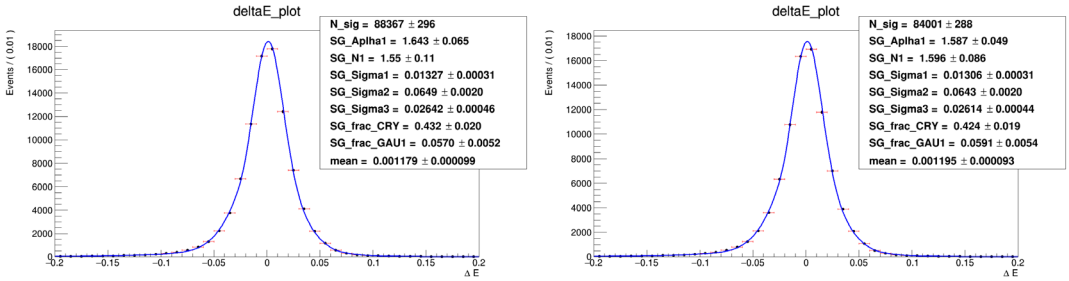

(a) (left) The ΔE distribution of the control sample before the selection

(b) (right) The ΔE distribution of the control sample after the selection

Fig 4.1 The ΔE distribution due to J/ψ decay angle selection on the control sample of $J/\psi\ K^{*+}$ in Monte Carlo

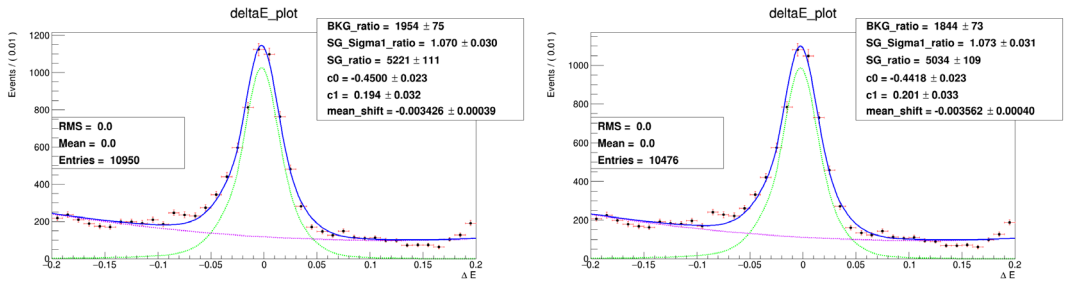

(a) (left) The ΔE distribution of the control sample before the selection

(b) (right) The ΔE distribution of the control sample after the selection

Fig 4.2 The ΔE distribution due to J/ψ decay angle selection on the control sample of $J/\psi\, K^{*+}$ in the Belle Data

	MC	Data	$\frac{Data}{MC}$
Without decay angle selection	88367 ± 296	5221 ± 111	
With decay angle selection	84001 ± 288	5034 ± 109	
ratio	0.9506 ± 0.0046	0.9642 ± 0.0292	1.0143 ± 0.0311

Table 4.8 The ratio of with and without decay angle selection and systematic error between Monte Carlo and Data for J/ψ selection.

The error of the J/ψ selection is 3.07%. The 3.07% is 0.0311/1.0143.

4.3 η selection

For the η, we cut the energy of γ. Both η and π^0 decay to $\gamma\gamma$, so we cut the energy of γ to improve the separation power. The results are shown as Table 4.9 and Table 4.10.

$\eta \to \gamma\gamma$	MC	data
Without E_γ selection	4299354	334160
$E_\gamma > 0.2\ GeV$	2247983	166644
Event ratio	0.5229	0.4987

Table 4.9 The event ratio between without E_γ selection and with $E_\gamma > 0.2\ GeV$ selection in Monte Carlo and Data for $\eta \to \gamma\gamma$ selection.

Systematic Error Calculation: $\frac{0.4987-0.5229}{0.5229} = 4.63\%$

$\pi^0 \to \gamma\gamma$	MC	data
Without p_{π^0} selection	8208295	445574
$p_{\pi^0} > 0.2$ GeV/c	7285927	420101
Event ratio	0.8876	0.9428

Table 4.10 The event ratio between without p_{π^0} selection and with $p_{\pi^0} > 0.2GeV/c$ selection in Monte Carlo and Data for $\pi^0 \to \gamma\gamma$ selection.

Systematic Error Calculation: $\frac{0.9428-0.8876}{0.8876} = 6.2\%$

4.4 Fitting

When we fit the PDF function on the Belle data, we fix the parameters of the signal PDF. We want to test the difference of the signal yields while floating the parameters. we shifted the mean and scaled the width, and we found the systematic error of the PDF fitting is 2.17%. The results are shown as Fig 4.3, Fig 4.4, Fig 4.5 and Fig 4.6.

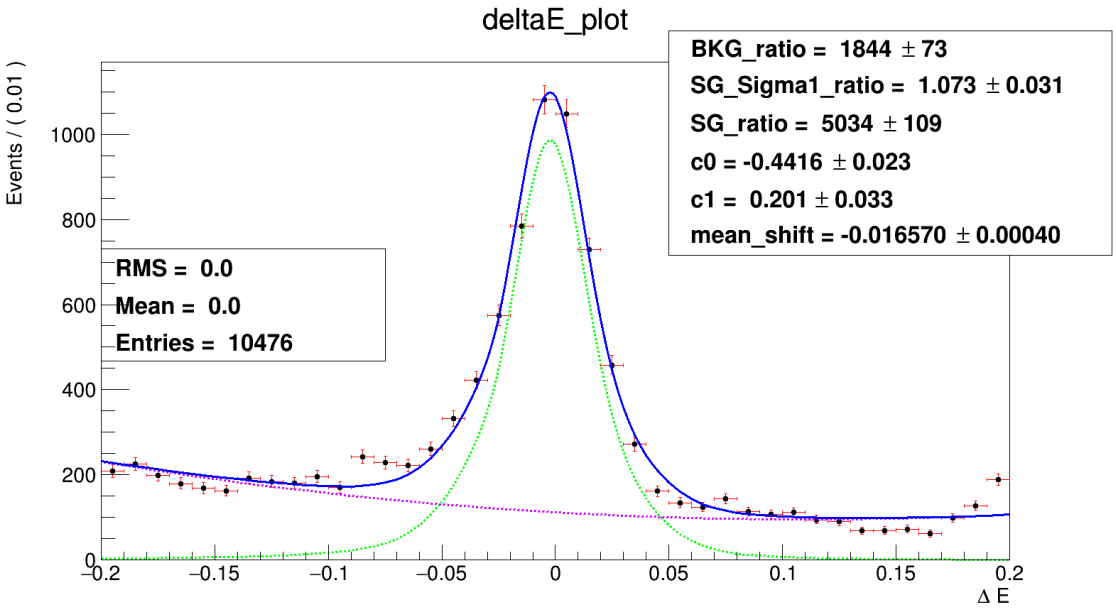

Fig 4.3 The ΔE distribution fitting result of the control sample when the mean value adds 1σ.

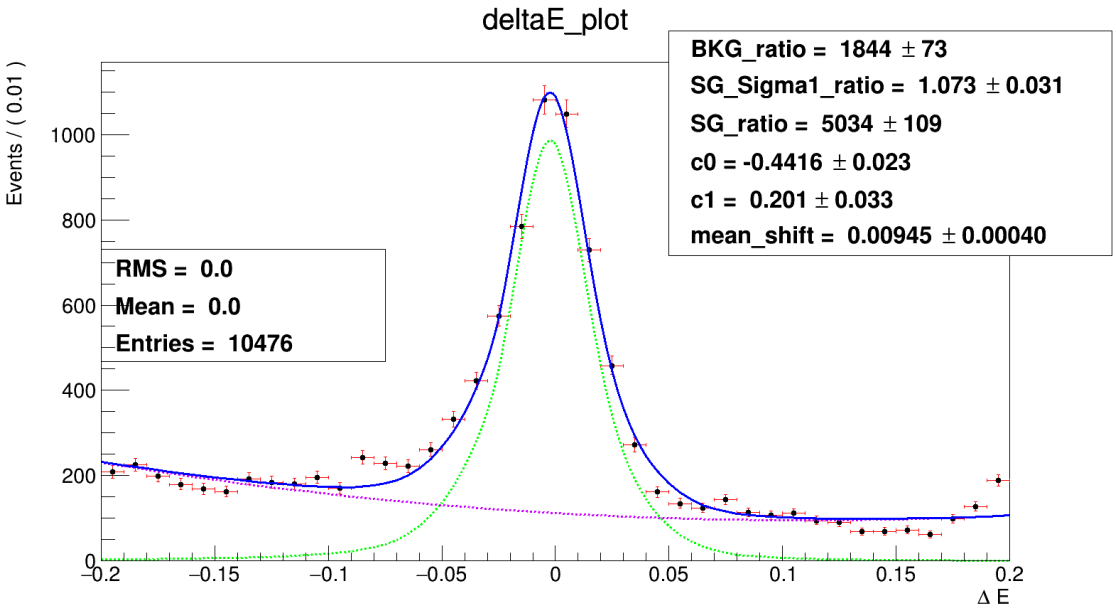

Fig 4.4 The ΔE distribution fitting result of the control sample when the mean value subtracts 1σ.

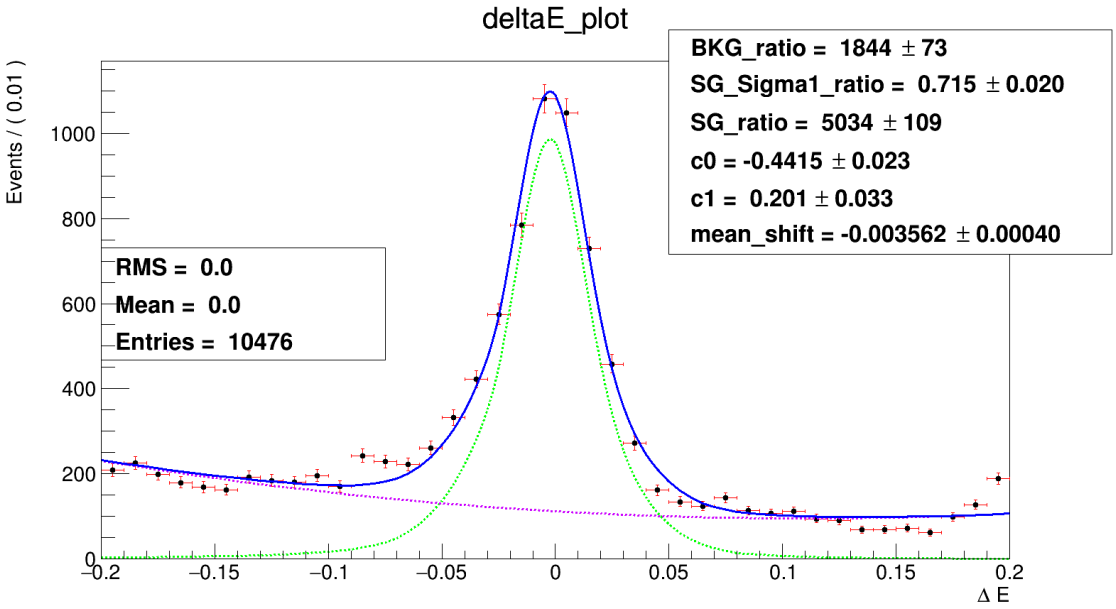

Fig 4.5 The ΔE distribution fitting result of the control sample with the widen width of 1.5σ.

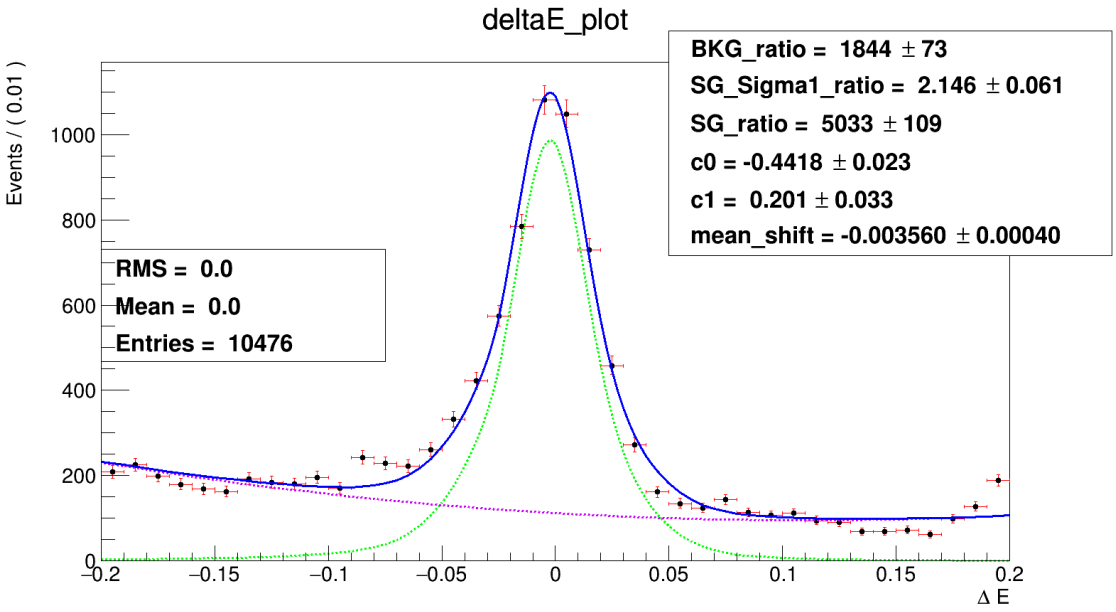

Fig 4.6 The ΔE distribution fitting result of the control sample with the narrowed width of 0.5σ.

4.5 Summary of the systematic errors

We summarized the systematic error in the decay $B^0 \to J/\psi\eta$ in our study and listed the systematic errors in Table 4.11.

	$J/\psi\eta(\to \gamma\gamma)$	$J/\psi\eta(\to \pi^+\pi^-\pi^0)$
$N(B\bar{B})$	1.37%	1.37%
Tracking (Charged particle)	$2 \times 0.35\%$	$4 \times 0.35\%$
KID	0	0.63% (π^+) 0.64% (π^-)
Lepton ID	1.45%(e^+) 1.46%(e^-) 2.02%(μ^+) 2.07%(μ^-) Average: 3.5% for two tracks	1.45%(e^+) 1.46%(e^-) 2.02%(μ^+) 2.07%(μ^-) Average: 3.5% for two tracks
J/ψ decay Angle	3.07%	3.07%
$\eta \to \gamma\gamma, \pi^0 \to \gamma\gamma$	4.63%	6.2%
PDF	2.17%	2.17%
$Br(J/\psi)$	1.11%	1.11%
$Br(\eta)$	0.51%	1.22%
Total Error	10.37%	12.24%

Table 4.11 The systematic error tables for $J/\psi\eta$.

Chapter 5 Open Data Box

5.1 Belle Data

Before open the data, we need to decide our signal PDFs, background PDFs, survey the background components. The needed branching fractions for the decays are shown on the PDG Website. We list the needed branching fraction in Table 5.1. The signal efficiencies are listed in Table 5.2.

We fix the signal PDF, background PDF and float the number of signal and background in the signal yield region. We get the branching fraction of $B^0 \to J/\psi\eta(\eta \to \gamma\gamma)$ is $(8.8 \pm 1.5 \pm 0.9) \times 10^{-6}$,the significance is 7.5σ. The branching fraction of $B^0 \to J/\psi\eta(\eta \to \pi^+\pi^-\pi^0)$ is $(17.6 \pm 5.2 \pm 2.2) \times 10^{-6}$, the significance is 4.7σ. We list the results in Table 5.3 and show the distributions as Fig 5.1 and Fig 5.2.

Meson	Branching fraction
$B^0 \to J/\psi\eta$	$(1.08 \pm 0.23) \times 10^{-5}$
$J/\psi \to e^+e^-$	$(5.971 \pm 0.032)\%$
$J/\psi \to e^+e^-\gamma$	$(8.8 \pm 1.4) \times 10^{-3}$
$J/\psi \to \mu^+\mu^-$	$(5.961 \pm 0.033)\%$
$\eta \to \gamma\gamma$	$(39.41 \pm 0.20)\%$
$\eta \to \pi^+\pi^-\pi^0$	$(22.92 \pm 0.28)\%$

Table 5.1 The branching fraction listed for each meson which get from PDG Website.

Decay Channel	Signal Efficiency (ϵ)
$J/\psi \to e^+e^-(\gamma), \eta \to \gamma\gamma$	16.755%
$J/\psi \to \mu^+\mu^-, \eta \to \gamma\gamma$	18.593%
$J/\psi \to e^+e^-(\gamma), \eta \to \pi^+\pi^-\pi^0$	4.473%
$J/\psi \to \mu^+\mu^-, \eta \to \pi^+\pi^-\pi^0$	4.732%

Table 5.2 The signal efficiency for each decay channel.

	Signal Yield	Branching Fraction	Significance
$\eta \to \gamma\gamma$	60 ± 10	$(8.8 \pm 1.5 \pm 0.9) \times 10^{-6}$	7.5σ
$\eta \to \pi^+\pi^-\pi^0$	18.3 ± 5.4	$(17.6 \pm 5.2 \pm 2.2) \times 10^{-6}$	4.7σ

Table 5.3 The signal yield, branching fraction and significance result for the $B^0 \to J/\psi\eta$ decay.

For $\eta \to \gamma\gamma$ mode:

$N_{s1} + N_{s2} = 60 \pm 10, Br(B^0 \to J/\psi\,\eta) = (8.7522 \pm 1.4587) \times 10^{-6}$

Significance: $-Log(\mathcal{L}_0) = -1348.31, -Log(\mathcal{L}_{Max}) = -1376.22$,

$$\sqrt{-2\ln\left(\frac{\mathcal{L}_0}{\mathcal{L}_{Max}}\right)} = 7.4713$$

For $\eta \to \pi^+\pi^-\pi^0$ mode:

$N_{s3} + N_{s4} = 18.3 \pm 5.4, Br(B^0 \to J/\psi\,\eta) = (17.596 \pm 5.1923) \times 10^{-6}$

Significance: $-Log(\mathcal{L}_0) = -353.063, -Log(\mathcal{L}_{Max}) = -363.912$,

$$\sqrt{-2\ln\left(\frac{\mathcal{L}_0}{\mathcal{L}_{Max}}\right)} = 4.6851$$

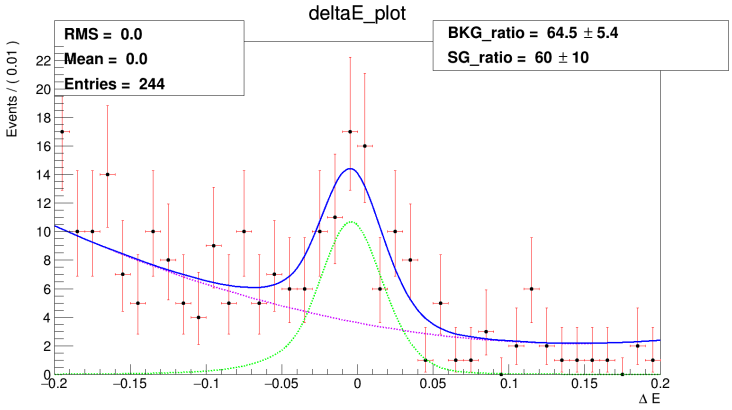

Fig 5.1 The ΔE distribution fitting result of data in the $\eta \to \gamma\gamma$ decay.

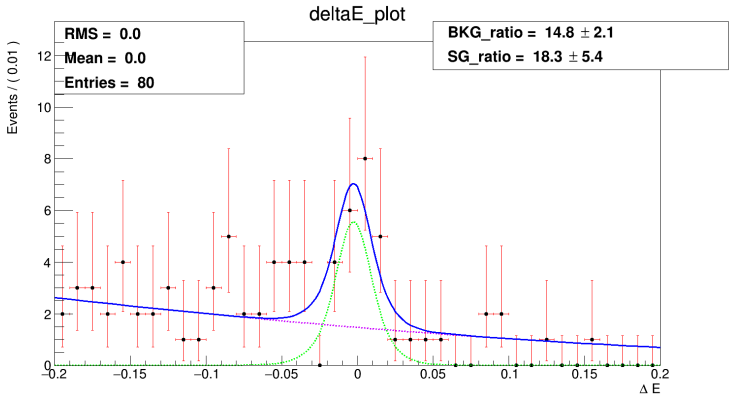

Fig 5.2 The ΔE distribution fitting result of data in the $\eta \to \pi^+\pi^-\pi^0$ decay.

5.2 Belle II Data

Currently, the number of $B\bar{B}$ in the Belle II Data cannot be enough to observe the $B^0 \to J/\psi\eta$ decay. Knowing from the result we have done in the control sample.

Chapter 6 Summary

6.1 The Branching Fraction of $B^0 \rightarrow J/\psi\eta$

In order to fit the result of the $\eta \rightarrow \gamma\gamma$ and $\eta \rightarrow \pi^+\pi^-\pi^0$ mode at the same time to get the signal yield in the signal region, we use the simultaneous PDF in the RooFit to fit two decay channels. To run the simultaneous fit, we fix the fraction between $\eta \rightarrow \gamma\gamma$ and $\eta \rightarrow \pi^+\pi^-\pi^0$.

The Branching fraction of $B^0 \rightarrow J/\psi\eta$ is $(10.9 \pm 1.6 \pm 1.2) \times 10^{-6}$. The significance is 8.7σ. The result is listed in Table 6.1. The simultaneous fit result is shown as Fig 6.1.

Signal Yield	Branching Fraction	Significance
86 ± 13	$(10.9 \pm 1.6 \pm 1.2) \times 10^{-6}$	8.7σ

Table 6.1 The signal yield, branching fraction and the significance of $B^0 \rightarrow J/\psi\eta$ decay.

$$-Ln(L_0) = -1476.8, \qquad -Ln(L_{MAX}) = -1515$$

$$\sqrt{-2\ln\left(\frac{\mathcal{L}_0}{\mathcal{L}_{Max}}\right)} = 8.7$$

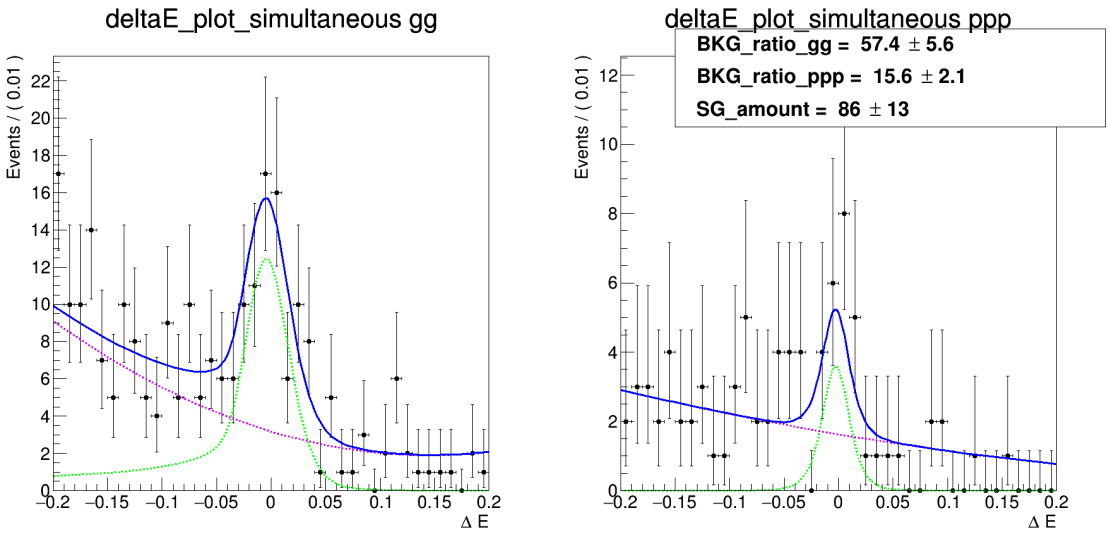

Fig 6.1 The ΔE distribution result of the simultaneous fit in the $B^0 \to J/\psi\eta$ decay.

6.2 Result comparison

The Branching fraction in "Observation of the decay $B^0 \to J/\psi\eta$ which published on Phys. Rev. Lett. 98, 131803 [1] is $\left(9.5 \pm 1.7(stat) \pm 0.8(syst)\right) \times 10^{-6}$. The significance is 8.1σ. The other result which published in Phys. Rev. D, "Measurement of $B^0 \to J/\psi\eta^{(\prime)}$ and constraint on the $\eta - \eta'$ mixing angle" [2] for the branching fraction is $\left(12.3 \pm \frac{1.8}{1.7} \pm 0.7\right) \times 10^{-6}$. The significance is 6.3σ. We compare the results in Table 6.2.

Result	Branching fraction	Significance
PRL 2007	$(9.5 \pm 1.7 \pm 0.8) \times 10^{-6}$	8.1σ
PRD 2012	$\left(12.3 \pm \frac{1.8}{1.7} \pm 0.7\right) \times 10^{-6}$	6.3σ
This thesis	$(10.9 \pm 1.6 \pm 1.2) \times 10^{-6}$	8.7σ

Table 6.2 The branching fraction comparison for PRL2007 PRD 2012 and this thesis.

Appendix A. Belle Data

The event number for each experiment as shown as the table as below.

Experiment Number	Millions of B-Pairs
7	6.4587 + 0.1615 - 0.0976
9	4.7597 + 0.0286 - 0.0473
11	8.8509 + 0.0517 - 0.0518
13	11.6998 + 0.2393 - 0.2392
15	13.5679 + 0.0963 - 0.1055
17	12.4588 + 0.3301 - 0.3301
19	27.1705 + 0.1676 - 0.1676
21	4.3371 + 0.0540 - 0.0676
23	6.4755 + 0.0675 - 0.0989
25	28.0008 + 0.3329 - 0.1605
27	28.1814 + 0.2110 - 0.1516
31	19.6587 + 0.3045 - 0.3031
33	19.3022 + 0.3000 - 0.2987
35	18.5262 + 0.2861 - 0.2855
37	67.1819 + 1.0326 - 1.0319
39	47.0818 + 0.7265 - 0.7246
41	64.0134 + 0.9863 - 0.9857
43	61.5614 + 0.9493 - 0.9474
45	14.3538 + 0.2218 - 0.2215
47	41.2186 + 0.6406 - 0.6393
49	29.7271 + 0.4648 - 0.4634
51	41.8919 + 0.6605 - 0.6590
55	80.2472 + 1.2462 - 1.2439

61	37.4460 + 0.5624 - 0.5617
63	35.6231 + 0.5297 - 0.5291
65	41.7867 + 0.6317 - 0.6309
Total Number of $B\overline{B}$ events	771.581 ± 10.566

Appendix B. Belle II Data

Processing Label	Experiment	Luminosity (offline) on resonance $\Upsilon(4S)$ [pb^{-1}]
		bhabha
proc11	7	425.5 ± 0.3
	8	4597.4 ± 0.9
	10	3741.3 ± 1.1
bucket9	12	2768.7 ± 1.1
bucket10	12	10361.1 ± 2.1
bucket11	12	12687.1 ± 2.3
bucket13	12	5055.1 ± 1.5

Appendix C.
Belle II Analysis Software Framework

release-04-02-04

light-2002-janus

1. BremsFinder

The module of BremsFinder will copies the each particle in the list of input to the output. The result of searching for the possible bremsstrahlung photons through the eclTrackBremFinder. If the result is matching to our decay, the four momentum of the particle will be added to the "outputlist".

The Bremsstranhlung weighted is determined as following

$$\max\left(\frac{|\phi_{clu}-\phi_{hit}|}{\Delta\phi_{clu}+\Delta\phi_{hit}},\frac{|\theta_{clu}-\theta_{hit}|}{\Delta\theta_{clu}+\Delta\theta_{hit}}\right)$$

ϕ_i and θ_i are the azimuthal and polar angles of the ECL Cluster and the extrapolated hit. Δ is the uncertainty of that value. This can be used in Belle II Analysis after MC12.

Bibliography

[1] Chang., M.C et al. (Belle Collab.), "Oberservation of the decay J/Ψη," *PRL 981131803,* p. 2, 2007.

[2] M.-C. Chang et al., "Measurement of B0 -> J/Ψ η (') and constraint on the η - η ' mixing angle," *Phys. Rev. D 85, 091102(R),* 4 May 2012.

[3] "Software Basf2 Introduction," [線上]. Available: https://confluence.desy.de/display/BI/Software+Basf2Introduction.

[4] T. Kuhr (et al Belle II Framework Software Group), "The Belle II Core Software," *BELLE2-PUB-TE-2018-002,* 2018.

[5] "EvtGen," [線上]. Available: https://evtgen.hepforge.org/. [存取日期: 13 1 2021].

[6] "Software EvtGen," [線上]. Available: https://confluence.desy.de/display/BI/Software+EvtGen.

[7] CERN, "ROOT," [線上]. Available: https://root.cern/about/. [存取日期: 13 1 2021].

[8] "RooFit," [線上]. Available: https://root.cern/manual/roofit/.

[9] M. Gelb, T. Keck, M. Prim, H. Atmacan, J. Gemmler, R. Itoh, B. Kronenbitter, T. Kuhr, M. Lubej, F. Metzner, C. Park, S. Park, C. Pulvermacher, M. Ritter 且 A. Zupanc, “B2BII - Data conversion from Belle to Belle II,” *arXiv:1810.00019,* 2018.

[10] “The Belle II Physics Book”.*arXiv:1808.10567.*

[11] “ Belle II Detector, ” [線 上]. Available: https://www.belle2.org/research/detector/.

[12] “ Source code for stdCharged, ” [線 上]. Available: https://software.belle2.org/sphinx/light-2008-kronos/_modules/stdCharged.html#stdCharged.

[13] J. Tanaka.*Belle Note 194 (unpublished).*

[14] C. Cecchi , G. De Nardoy and M. Merola, E. Manonix and A. Selce{, “Approved plots of R2 distribution in Early Phase 3 Data,” *BELLE2-NOTE-PL-2019-013,* 18 July 2019.

[15] R.Itpj, *BN 487,* 2001.

[16] “ Belle Systematic, ” [線 上]. Available: https://belle.kek.jp/secured/wiki/doku.php?id=software:systematics. [存取日期: 1 2 2021].

[17] “Number of B events in Hardon B(J),” 2009. [線上]. Available: https://belle.kek.jp/secured/nbb/nbb.html. [存取日期: 13 1 2021].

[18] “Belle Systematic Estimation for kid,” [線上]. Available: https://belle.kek.jp/group/pid_joint/kid/kid.html.

[19] “Systematic Estimation Lepton ID,” [線上]. Available: https://belle.kek.jp/group/pid_joint/lid/lid.html. [存取日期: 1 Feb 2021].